THE OPERATION OF ROTATING NON-CAPILLARY HEAT PIPES

John Sanford Woodard

NAVAL POSTGRADUATE SCHOOL
Monterey, California

THESIS

THE OPERATION OF ROTATING NON-CAPILLARY HEAT PIPES

by

John Sanford Woodard

Thesis Advisor: P. J. Marto

March 1972

The Operation of Rotating Non-Capillary Heat Pipes

by

John Sanford Woodard
Lieutenant Commander, United States Navy
B.S., United States Naval Academy, 1960

Submitted in partial fulfillment of the
requirements for the degree of

MASTER OF SCIENCE IN MECHANICAL ENGINEERING

from the

NAVAL POSTGRADUATE SCHOOL
March 1972

ABSTRACT

A Nusselt-type analysis was performed for laminar film condensation on the inside of a truncated rotating cone, which included the interfacial shear between the vapor and condensate, the vapor pressure drop, the thermal resistance in the condenser wall, and the condenser exterior cooling mechanism. An approximation of this analysis made it possible to find a numerical solution for small half cone angles greater than zero. A parametric study was performed of this approximate solution for various fluids, RPMs, half cone angles, and exterior heat transfer coefficients.

A non-capillary rotating heat pipe containing distilled water as the working fluid was tested. It was rotated at 700, 1400, 2100, and 2800 RPM, and heat transfer rates of the heat pipe were determined experimentally for different vapor saturation temperatures corresponding to electrical power inputs ranging from 1 Kw to 7 Kw.

The experimental results showed that the heat pipe performance was influenced by non-condensible gases in the working fluid and suggested that the analytical solution predicted heat transfer rates which were too high.

TABLE OF CONTENTS

TABLE OF SYMBOLS

A_c	surface area of condenser, ft^2
c_p	specific heat, Btu/lb_m - °F
f	friction factor, dimensionless
h	external heat transfer coefficient, Btu/hr - ft^2 - °F
h_{fg}	latent heat of evaporation, Btu/lbm
k_f	thermal conductivity of the liquid, Btu/hr - ft - °F
k_w	thermal conductivity of condenser wall, Btu/hr - ft - °F
L_c	length of condenser, ft
$\dot{m}$	mass flow rate of coolant, lbm/hr
p_v	pressure of the vapor, lbf/ft^2
Q	theoretical heat transfer rate out of heat pipe, Btu/hr
$\dot{Q}_{OUT}$	total experimental heat transfer rate out of heat pipe, Btu/hr
R	internal condenser radius, ft
R_o	minimum internal radius of condenser, ft
T_s	vapor saturation temperature, °F
T_∞	inlet coolant temperature, °F
t	condenser wall thickness, ft
u	velocity of liquid, ft/sec
v	velocity of vapor, ft/sec
x	coordinate measuring distance along condenser

GREEK

δ	film thickness, ft
ϕ	half cone angle, radians
ρ_f	density of the liquid, lbm/ft^3
ρ_v	density of the vapor, lbm/ft^3
τ	shear stress, lbf/ft^2
μ_f	viscosity of the liquid, lbm/ft - sec
μ_v	viscosity of the vapor, lbm/ft - sec
ω	angular velocity, rad/sec

I. INTRODUCTION

A. THE ROTATING NON-CAPILLARY HEAT PIPE

The rotating non-capillary heat pipe is a closed rotating container capable of transferring large amounts of heat at nearly isothermal conditions. It consists of three main parts: (1) evaporator, (2) condenser, and (3) working fluid. When the heat pipe is rotated above a critical RPM the working fluid forms an annulus in the evaporator. The working fluid is evaporated in that section of the heat pipe by some heat source. As the vapor pressure increases, the vapor flows toward the condenser end, transporting the latent heat of vaporization. The latent heat is removed from the vapor as it condenses at the condenser end of the heat pipe. The condensate is then returned to the evaporator section of the heat pipe.

B. BACKGROUND

Ballback's study [ref. 2] of the rotating heat pipe indicated that its heat transfer capability is limited by the amount of heat which can be removed from the condenser. In his study, Ballback performed a Nusselt-type analysis for film condensation on the inside of a rotating truncated cone. In order to obtain a closed form solution for the condensate film thickness, δ, he made the following assumptions: (1) the rate of change of film thickness with a change in position along the condenser in the direction of the evaporator, $\frac{d\delta}{dx}$, was much less than the tangent of the half cone angle of the condenser, tan ϕ, (2) there were no shear stresses between the vapor and the condensate, and (3) there was no thermal resistance in the condenser wall. Daley, [ref. 3] was able to improve on the theory introduced by Ballback by taking into consideration the thermal

resistance in the condenser wall and the outside cooling mechanism. Furthermore, Daley neglected the assumption that $\frac{d\delta}{dx} << \tan \phi$. Using the velocity profile for the condensate developed by Ballback, he arrived at a non-linear second order differential equation for the film thickness, δ. Daley numerically integrated this expression using a Runge-Kutta-Gill numerical integration scheme with an IBM 360 MOD 67 digital computer. To start the integration, he used the conditions that $\delta = \delta_i$ and $\frac{d\delta}{dx} = \tan \phi$ at $X = 0$. It was postulated that δ_i was a function of the over-fall condition at the step located at the condenser exit. Daley arrived at an expression for the minimum film thickness, δ_m, at the condenser exit, using the approximation that the flow over the step approximated the free fall condition for open channel flow. Having found the film thickness from the second order differential equation at $X = L_c$, the condenser exit, Daley compared this value with δ_m at L_c. When the difference was less than 0.0004 inches, a solution was found. Using this technique, Daley was able to find the heat flow out of the condenser as a function of RPM for a 0° half cone angle only. As the cone angle was increased, however, the non-linear second order differential equation for the condensate film thickness became extremely sensitive to the initial value of the film thickness. Consequently, no solutions were found for the condensate film thickness for half cone angles greater than zero. Newton's study [ref. 5] continued to improve on Ballback and Daley by including the effects of vapor pressure drop and interfacial shear stress between the liquid and the vapor. Newton also considered thermal resistance of the condenser wall and the outside cooling mechanism. Newton then reduced his problem to a system of two first order differential equations which produced solutions for half cone angles of 0°, 0.1°, 0.2°,

and 0.3°. From the above solutions he found that $\frac{d\delta}{dx} << \tan\phi$. An approximate solution using this assumption and using as an initial condition $\delta = 0$, was tried with success. The solution which resulted from this approximation deviated less than 2.4% from the numerical solution. In addition it was conservative in its estimate of the heat transfer rate. The agreement between this approximate solution and the exact solution improved as half cone angle increased.

Newton then operated the heat pipe designed and assembled during Daley's study and made some initial comparisons of the analytical and experimental results. His experimental results, which contained a large uncertainty due to the parameter measurement techniques, indicated that the heat pipe was transferring on the order of 20% more energy than the theoretical analysis predicted. Visual observation of the heat pipe in operation showed definitely that film condensation was not achieved. Efforts made to achieve wetting of the stainless steel condenser section by the water, and therefore film condensation, were unsuccessful. The dropwise condensation mechanism which was achieved, with its known improvement in heat transfer ability, was the suggested primary reason for the deviation of the experimental results from the analytical solution. Time limitations also prevented Newton from performing any analysis on his approximate solution to predict the performance of the heat pipe over a wide range of conditions.

C. THESIS OBJECTIVES

The objectives of this study were therefore to: (1) conduct a parametric study of the analytical solution developed by Newton, (2) improve the instrumentation and operational equipment and procedures of the heat pipe to obtain more reliable experimental data, and (3) compare the analytical and experimental results.

II. THEORETICAL PROGRAM

A. REVIEW

The Nusselt type film condensation analysis performed by Ballback and Daley was extended by Newton to include the effects of vapor pressure drop, interfacial shear, thermal resistance in the condenser wall and outside cooling mechanism. Equations for momentum, continuity and energy were developed for an infinitesimal fluid element in the condensate, and, assuming one dimensional turbulent flow, momentum and continuity equations were developed for isothermal vapor flow. The details of the reduction of these equations can be found in Newton's thesis [ref. 5]. The reduction did result however in the system of simultaneous first order differential equations

$$\frac{dv}{dx} = \frac{2(R_o + x\sin\phi)(T_s - T_{o})}{\rho_v\left[\frac{\delta}{k_f} + \frac{t}{k_w} + \frac{1}{h}\right]R^2 h_{fg}} - \frac{2v}{R}\left[\sin\phi - \cos\phi\frac{d\delta}{dx}\right] \qquad (1)$$

and

$$\frac{d\delta}{dx} = \tan\phi - \frac{\rho_v V^2 f\left[\frac{P_1}{R} + \frac{P_2}{2}\right] + \rho_v v\left[\frac{\Delta R}{2\rho_f} - 2P_1\frac{dv}{dx}\right]}{P_1\cos\phi\left[\rho_f\omega R + \frac{2\rho V^2}{R}\right]} \qquad (2)$$

where

$$P_1 = (R_o + x\sin\phi)\frac{\delta^3}{3} - \cos\phi\frac{5}{24}\delta^4$$

$$P_2 = (R_o + x\sin\phi)\frac{\delta^2}{2} - \cos\phi\frac{\delta^3}{3}$$

A Runge-Kutta numerical integration was used to solve the equations simultaneously with the IBM computer. The solution of these equations depended on assuming an initial value of δ which was satisfactory for half cone angles less than 0.3°. However, the solution became extremely sensitive to initial values of δ at angles greater than this. As it was, in order to find the solution for 0.3°, 10,000 steps were necessary in the integration. He noted that $\frac{d\delta}{dx} << \tan\phi$. When this approximation was used in equations (1) and (2), they reduced to the equations

$$\frac{dv}{dx} = \frac{2(R_o + x\sin\phi)(T_s - T_\infty)}{\rho_v\left[\frac{\delta}{k_f} + \frac{t}{k_w} + \frac{1}{h}\right] R^2 h_{fg}} - \frac{2v\sin\phi}{R} \tag{3}$$

and

$$\delta^3 R\sin\phi\left[\rho_f\omega^2 R + \frac{2\rho_v v^2}{R}\right] - \rho_v v^2 f\left[R\frac{\delta^2}{4}\right] - \rho_v v\,\frac{\mu_f R^2}{2\rho_f} = 0 \tag{4}$$

Equation (3) was numerically integrated, using 1000 steps of integration over the cooling length of the condenser. Initial values of $\delta = 0$, and $v = 0$ at $x = 0$ were used to start the integration. The value of vapor velocity, $v(x)$, found at each integration step was used in the solution of equation (4) for $\delta(x)$. This value of $\delta(x)$ was then used in the next step of the integration of equation (3). After all values of δ were found, the equation

$$\frac{dQ(x)}{dx} = (T_s - T_\infty)\,\frac{2\pi(R_o + x\sin\phi)}{\frac{\delta(x)}{k_f} + \frac{t}{k_w} + \frac{1}{h}} \tag{5}$$

was integrated over the length of the condenser, L_c, to find the total heat transfer rate of the heat pipe. Solutions to this system of equations were within 2.4% of the exact solution for half cone angles up to 0.3°.

For half cone angles greater than 0.3° this approximation yielded solutions which were independent of the initial value of δ and required much less computation time.

B. PARAMETRIC STUDY

Since agreement between the exact solution and the approximate solution was satisfactory and the approximate solution was much easier to use, in that it did not require an initial search for starting condensate film thickness, especially for half cone angles greater than 0.3°, a parametric study of the heat pipe operating characteristics was performed using this approximate solution.

Clear cut relationships between equipment response and individual parameters are very useful for the engineering designer. In an attempt to establish these relationships a preliminary dimensional analysis was performed on the approximate system of equations which led to the functional relation

$$\frac{Q}{k_f L_c (T_s - T_\infty)} = f\left[\frac{L_c \sin\Phi}{R_o}, \frac{\omega R_o^2}{\nu_f}, \frac{k_w}{k_f}, \frac{t}{R_o}, \frac{hR_o}{k_f}, \frac{\rho_v}{\rho_f}, \frac{\mu_v}{\mu_f}, \frac{P_r}{c_p \Delta T / h_{fg}}, \frac{\mu_f}{\rho_f R_o \sqrt{h_{fg}}}\right] \qquad (6)$$

where $\frac{Q}{k_f L_c (T_s - T_\infty)}$ is a non-dimensional form of the heat transfer rate of the heat pipe.

The interdependence of the nine non-dimensional parameters made evaluation of the effects of these parameters unproductive. Since the problem could be reduced to one of separating the independent operational variables into broad categories of (1) working fluid and its properties, (2) rotational speed of the heat pipe, (3) exterior heat transfer coefficient, and (4) geometry, convenient parameters from these categories were selected to be studied.

Since the experimental model was instrumented to measure the saturation temperature of the vapor, T_s, this parameter was chosen as one of the variables of the parametric study. The selection of RPM as an independent operational parameter to vary in this study needs no explanation. The condenser cooling mechanism, represented by the exterior heat transfer coefficient, h, is determined by conditions which can be made independent of the internal configuration of the heat pipe, the working fluid selected, and the rate of heat pipe rotation. Therefore, h was selected as variable to be studied. The selection of a geometric parameter to vary was more difficult due to the inter-related nature of internal radius, R_o, condenser length, L_c, and half cone angle, ϕ. R_o and ϕ were arbitrarily selected for this area of study.

During the study, RPM was varied in increments of 600 RPM from 600 RPM to 3600 RPM. Values of h used were 50, 100, 500, 1000, 3000, and 10^{15} BTU/HR-ft^2-°F units (the last in order to approximate an infinite heat transfer coefficient). The fluids used were water, ethyl alcohol and Freon 113, since these fluids have satisfactory liquid and vapor properties in the range of conditions studied, and have been used by other researchers enough to provide some comparison with previous research in the field of condensation.

The analytical results are presented in tabular form in Appendix C. All graphs with one exception, the plot of heat transfer rate vs half cone angle, are plotted with the saturation temperature of the fluid on the abscissa and the heat transfer rate of the heat pipe on the ordinate. In this manner, heat pipe response is plotted as a function of the fluid properties with all other parameters held constant for a specific curve.

In each figure, one additional parameter, RPM, h, or ϕ, was varied producing a family of curves, thereby illustrating the effects of varying that parameter on the response of the heat pipe.

C. DISCUSSION OF ANALYTICAL RESULTS

In actual operation, the heat transfer rate required of the heat pipe is determined by its application. The equilibrium saturation temperature at which the pipe will operate is then reached for the other conditions of the pipe. Figure 1 shows the response of the pipe to the overall physical properties of the specific fluid in use. Water, in the range of operation studied is obviously the most satisfactory fluid. Its high latent heat of vaporization, 3 times that of alcohol, and 15 times that of Freon 113, and its high thermal conductivity relative to that of alcohol and Freon 113, would explain this difference in response.

Ballback's analysis indicated that the heat pipe response is proportional to the square root of the RPM. This response is modified in the analysis by the existance of thermal resistance in the condenser wall and the thermal resistance of the external heat transfer coefficient. However, analysis of the data in Table 1 indicates that the heat pipe response approaches this theoretical relationship, $Q \propto \omega^{1/2}$, as the exterior heat transfer coefficient becomes very, very large. Since Figures 2, 7, and 10 are plotted with a nominal exterior heat transfer coefficient of 1000, they only suggest this trend. They do, however, illustrate the heat pipe response with a more realistic exterior heat transfer coefficient.

Figures 3, 8, and 11 suggest the dependance of the heat pipe response on the condenser cooling mechanism, and a further comparison with the curves for other RPMs in the previous figures supports this suggestion.

At the low exterior heat transfer coefficients, very little difference is seen between the effectiveness of the various fluids. Thus it can be seen that the exterior heat transfer rate dominates the heat pipe response when the exterior heat transfer mechanism is poor. Figures 4, 9, and 13 further suggest the previous conclusion in that at low exterior heat transfer coefficients a change in half cone angle causes little change in heat pipe response. Quantitively, when the exterior heat transfer coefficient is 50 BTU/HR-ft^2-°F and the half cone angle is increased from 1° to 3° there is an 18% increase in the heat pipe response for all three fluids. However, at a heat transfer coefficient of 500 BTU/HR-ft^2-°F the heat pipe response increases 35% for the same change in half cone angle.

From Figure 5 it appears that after an initial rapid increase in response with increasing half cone angle, from 0° to 1°, for a nominal RPM and h, the relation approaches an approximate 17% increase in heat transfer rate per degree increase in half cone angle for the half cone angles investigated. Figure 5 also shows that there is a significant heat transfer rate even when there is no internal taper to the condenser.

The change of heat pipe response with change in internal radius is illustrated by Figure 6. The heat pipe response is related to the radius by two mechanisms. The direct relationship between heat pipe response and condenser area is evident from Equation (5). The change in centrifugal accelerations at the condensate film with a change in radius with its resultant change in condensate film thickness in addition to the area effect is suggested by Figure 6.

D. SUMMARY OF ANALYTICAL RESULTS

1. The interdependence of the various dimensionless parameters associated with the heat pipe precludes establishing convenient functional relationships between heat pipe response and any single parameter.

2. Heat pipe response is dominated by the exterior heat transfer mechanism when this mechanism leads to low exterior heat transfer coefficients.

3. The heat transfer rate of the heat pipe approaches a function of the square root of RPM for efficient exterior heat removal mechanisms.

4. There is a significant heat transfer rate with a 0° half cone angle. After an initial rapid rise with half cone angles from 0° to 1°, the heat transfer rate continues to increase with increasing half cone angles.

5. A change in internal radius has a relatively large effect on heat pipe response.

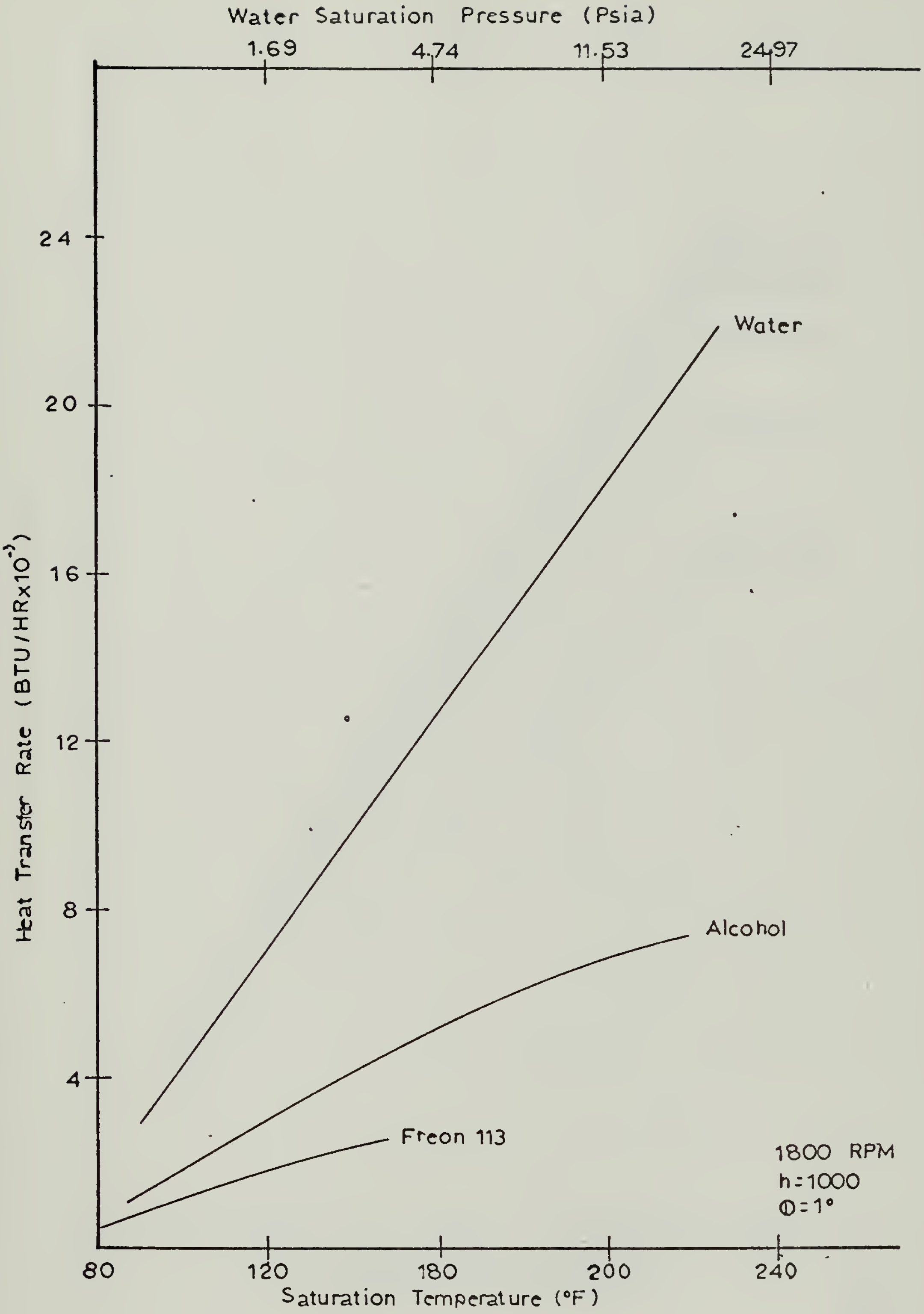

Fig. 1 Heat Pipe Response vs. Saturation Temperature for Water, Alcohol, and Freon 113

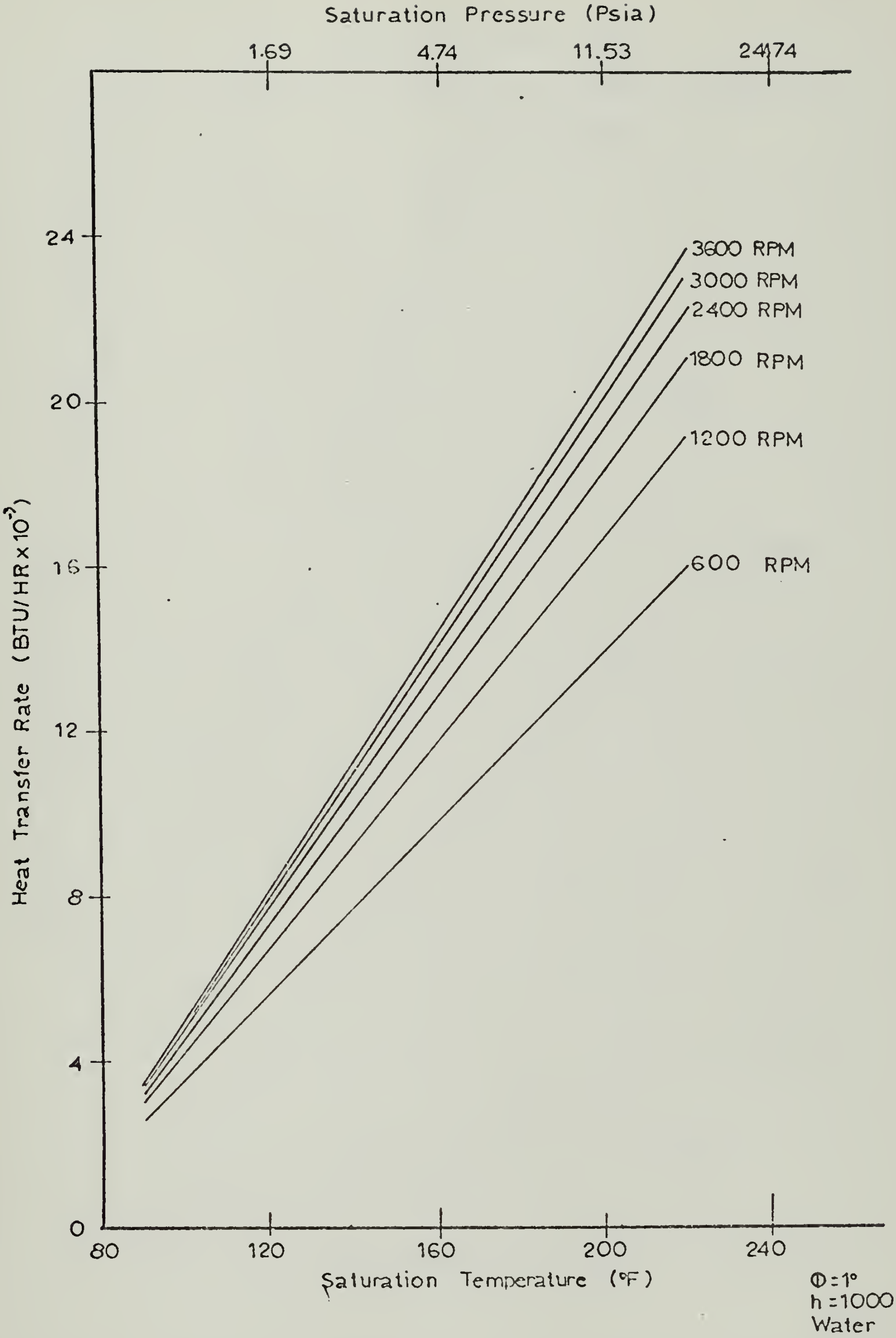

Fig. 2 Heat Pipe Response vs. Saturation Temperature for Water at various Rotating Speeds

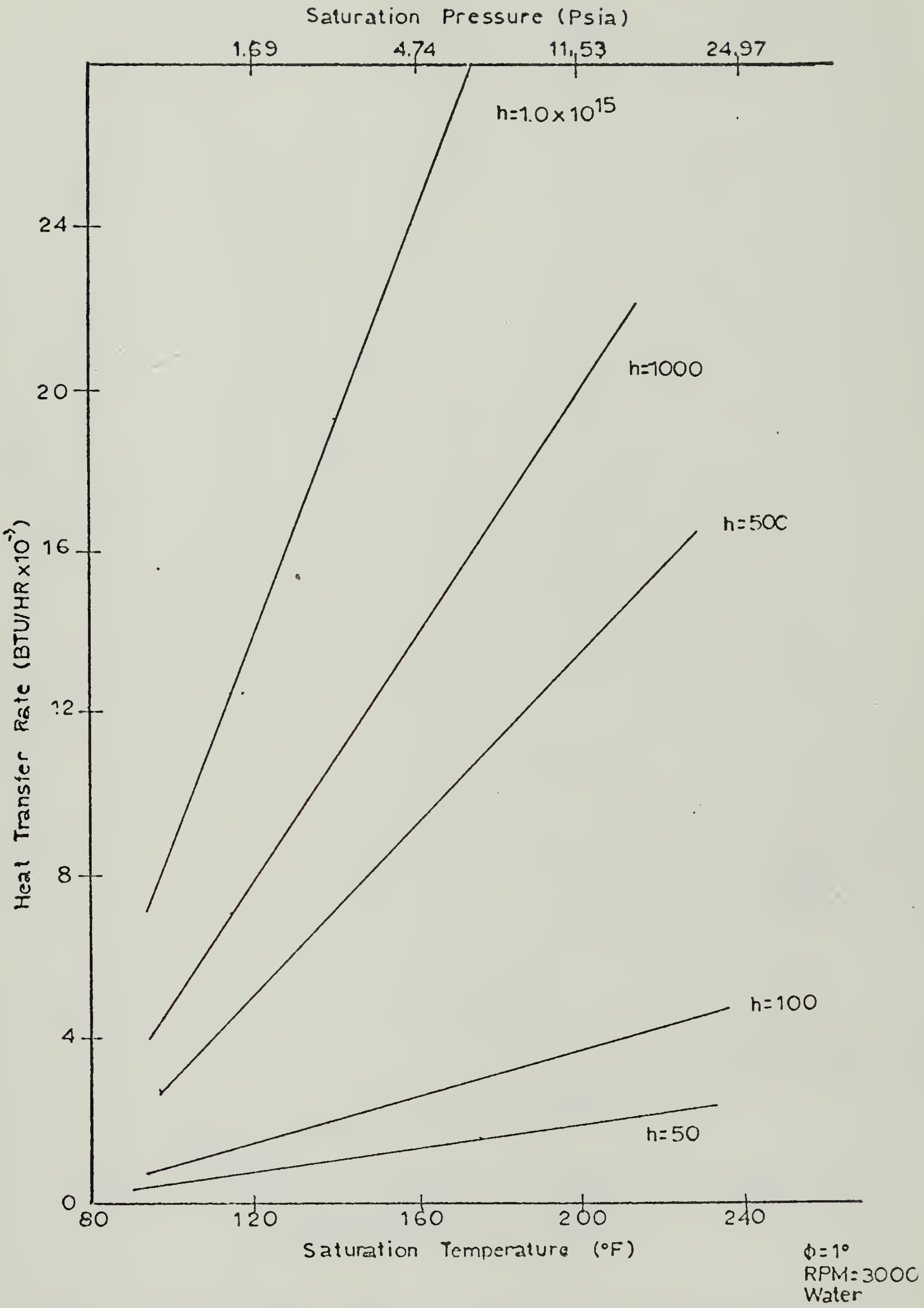

Fig. 3 Heat Pipe Response vs. Saturation Temperature for Water at various External Heat Transfer Coefficients

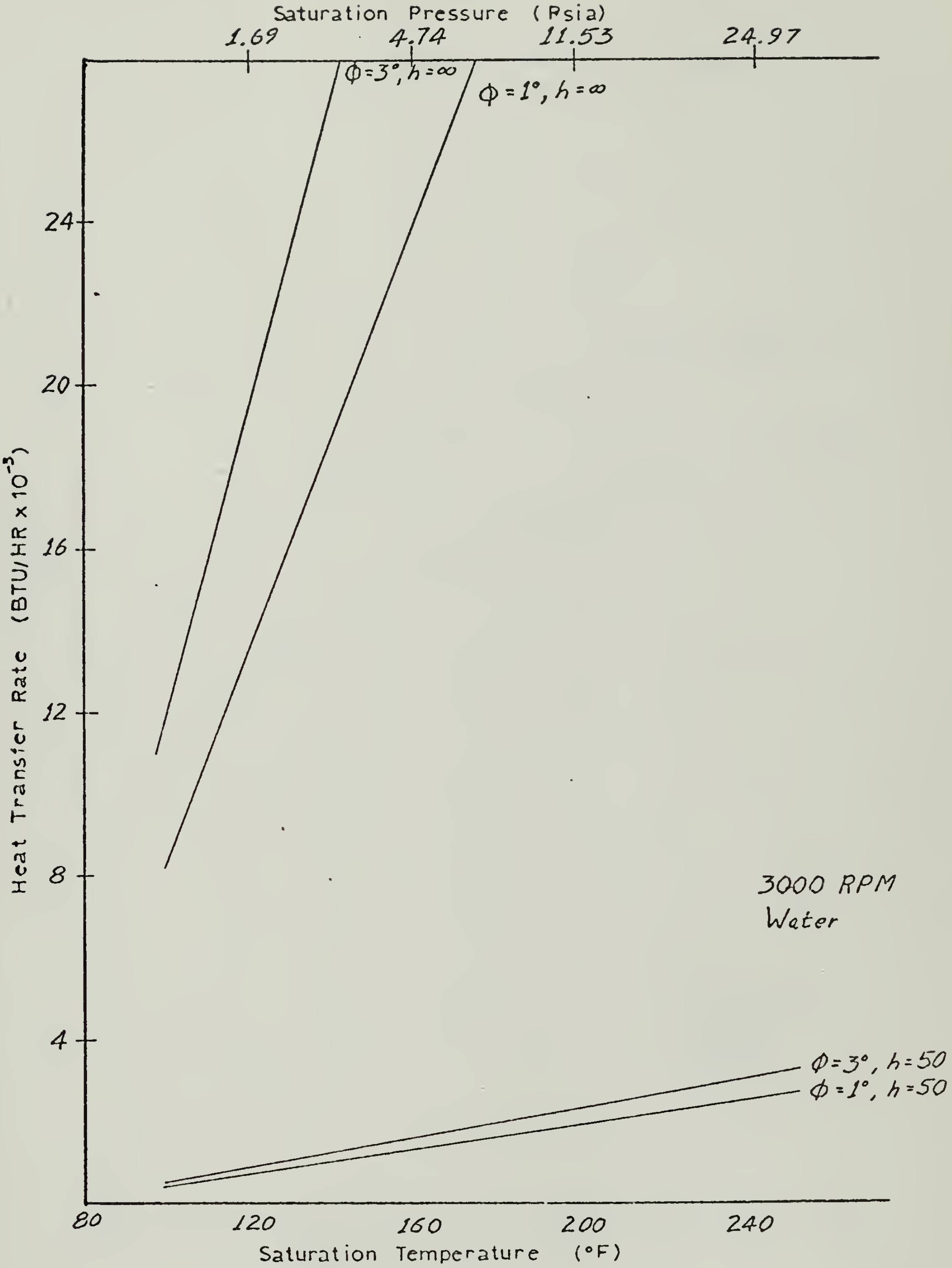

Fig. 4 Heat Pipe Response vs. Saturation Temperature for Water at two half cone angles and two exterior heat transfer coefficients

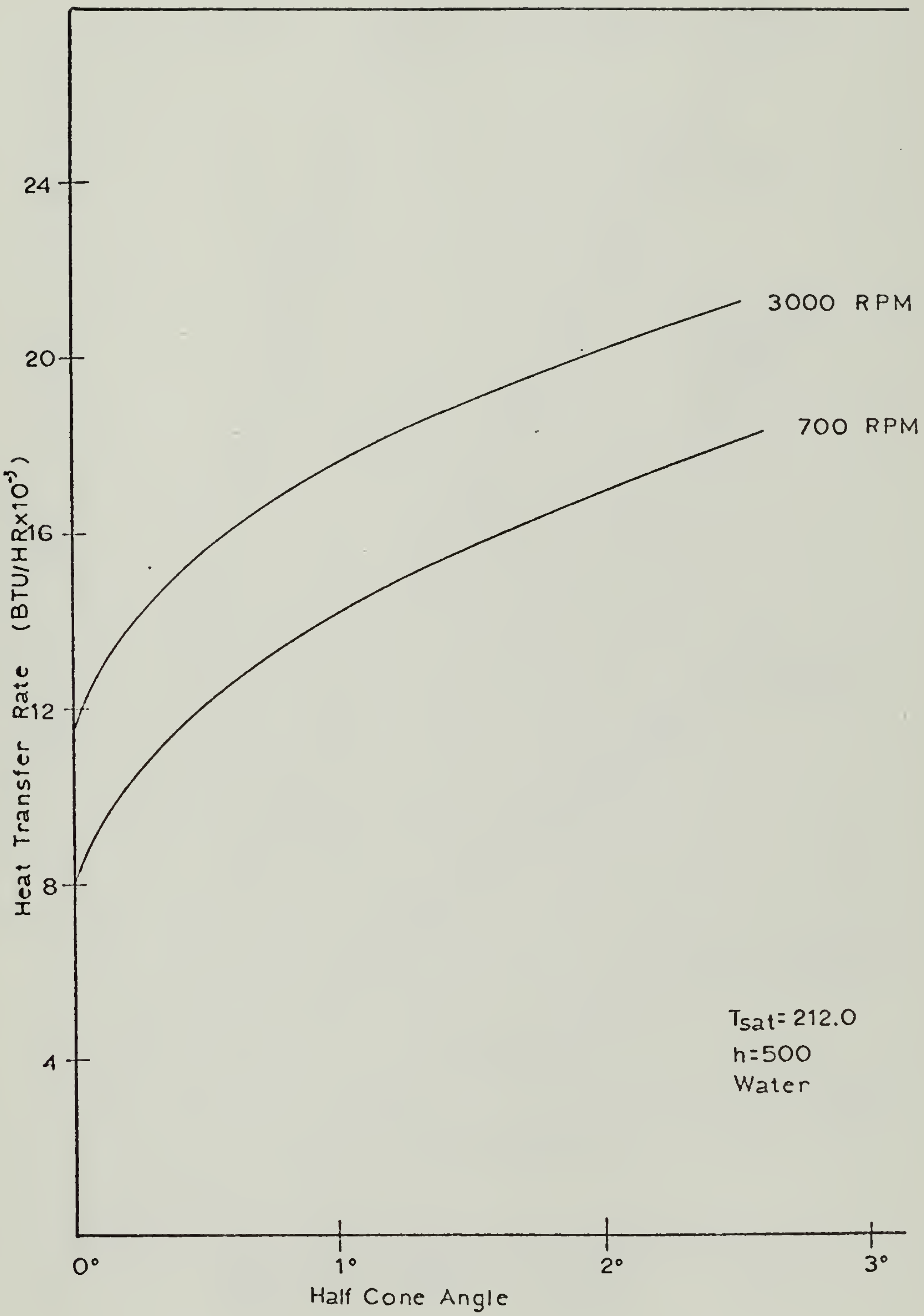

Fig. 5 Heat Pipe Response vs. Half Cone Angle for Water at two Rotating Speeds

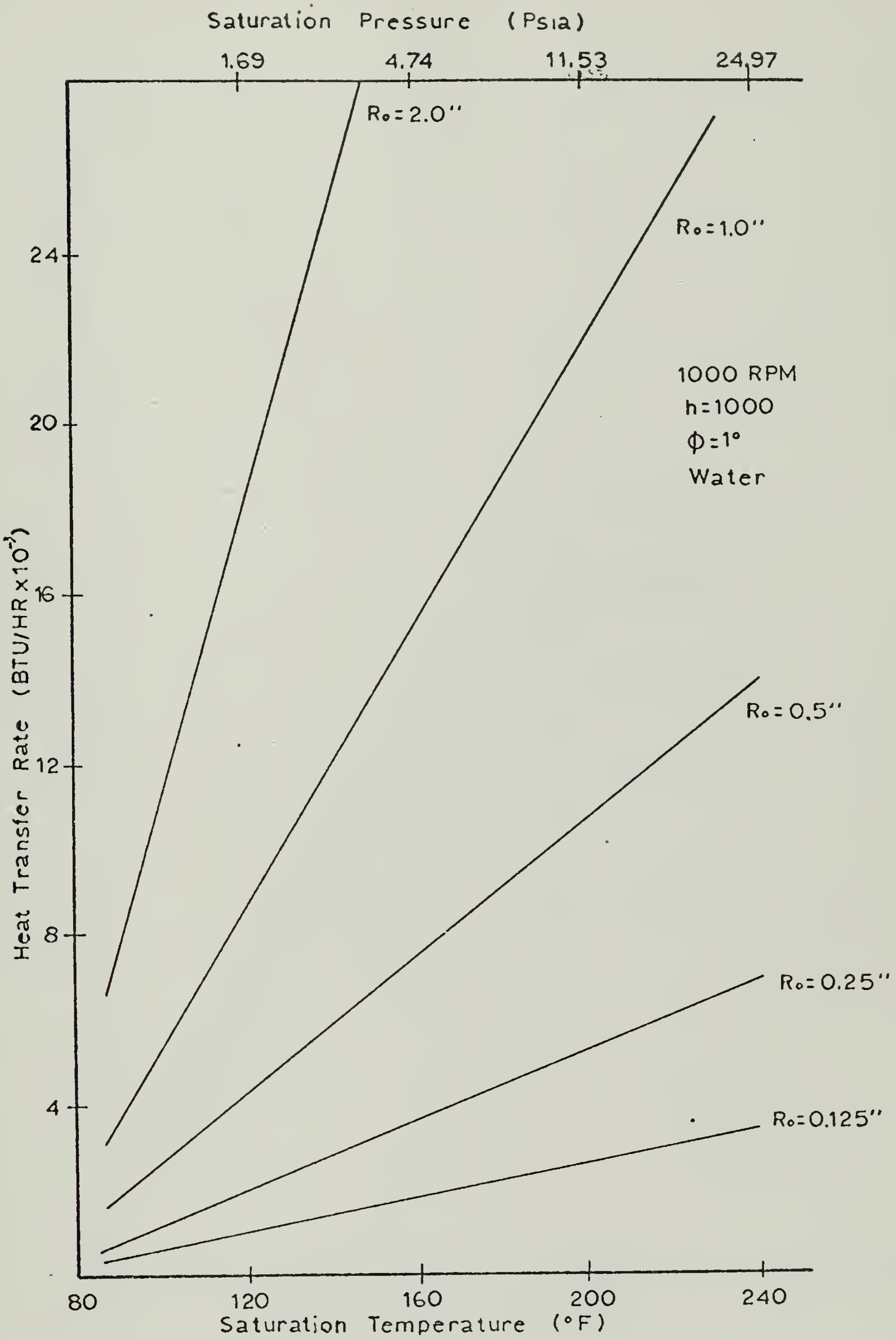

Fig. 6 Heat Pipe Response vs. Saturation Temperature for Water at various Internal Condenser Radii

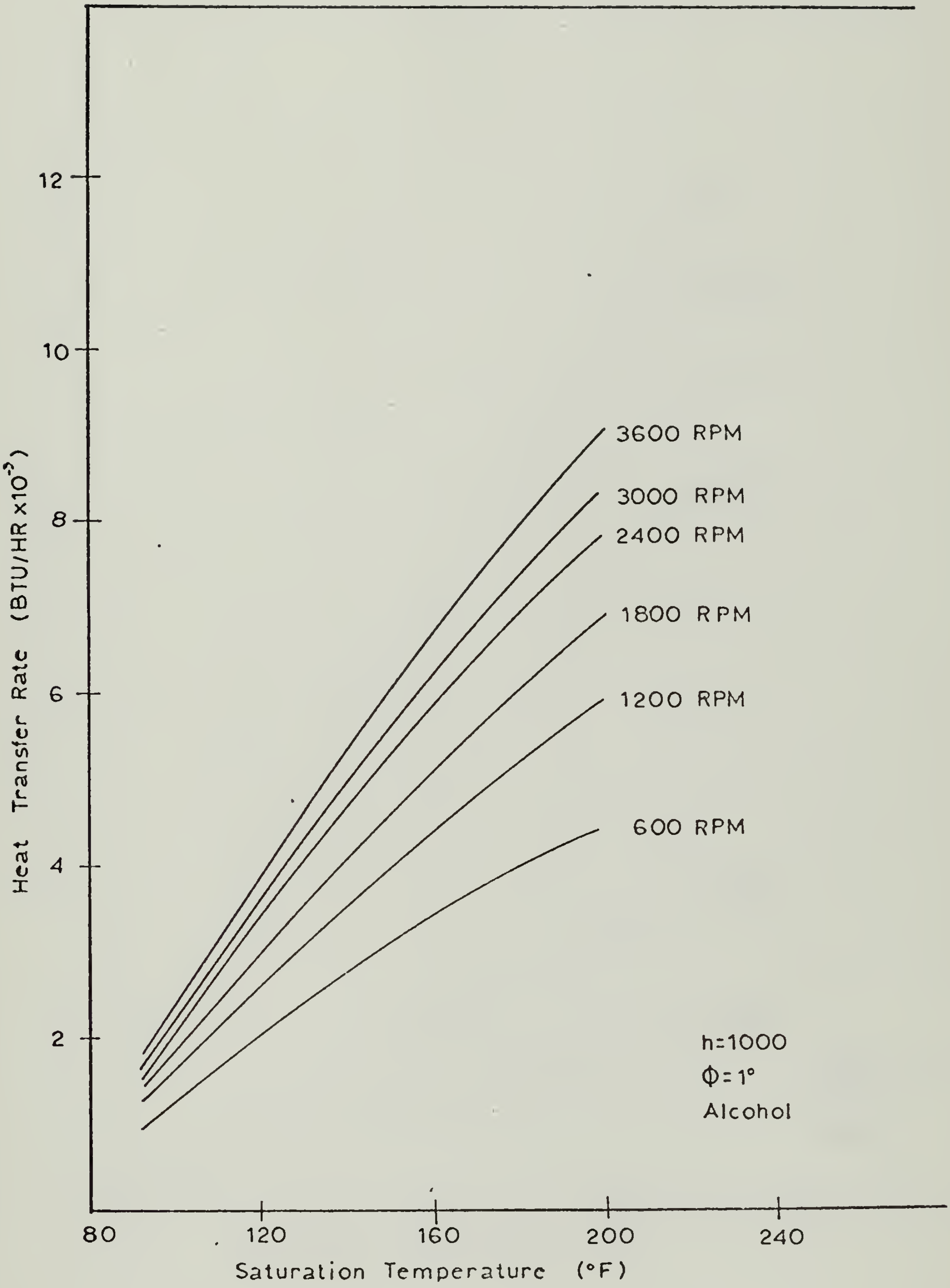

Fig. 7 Heat Pipe Response vs. Saturation Temperature for Alcohol at various Rotating Speeds

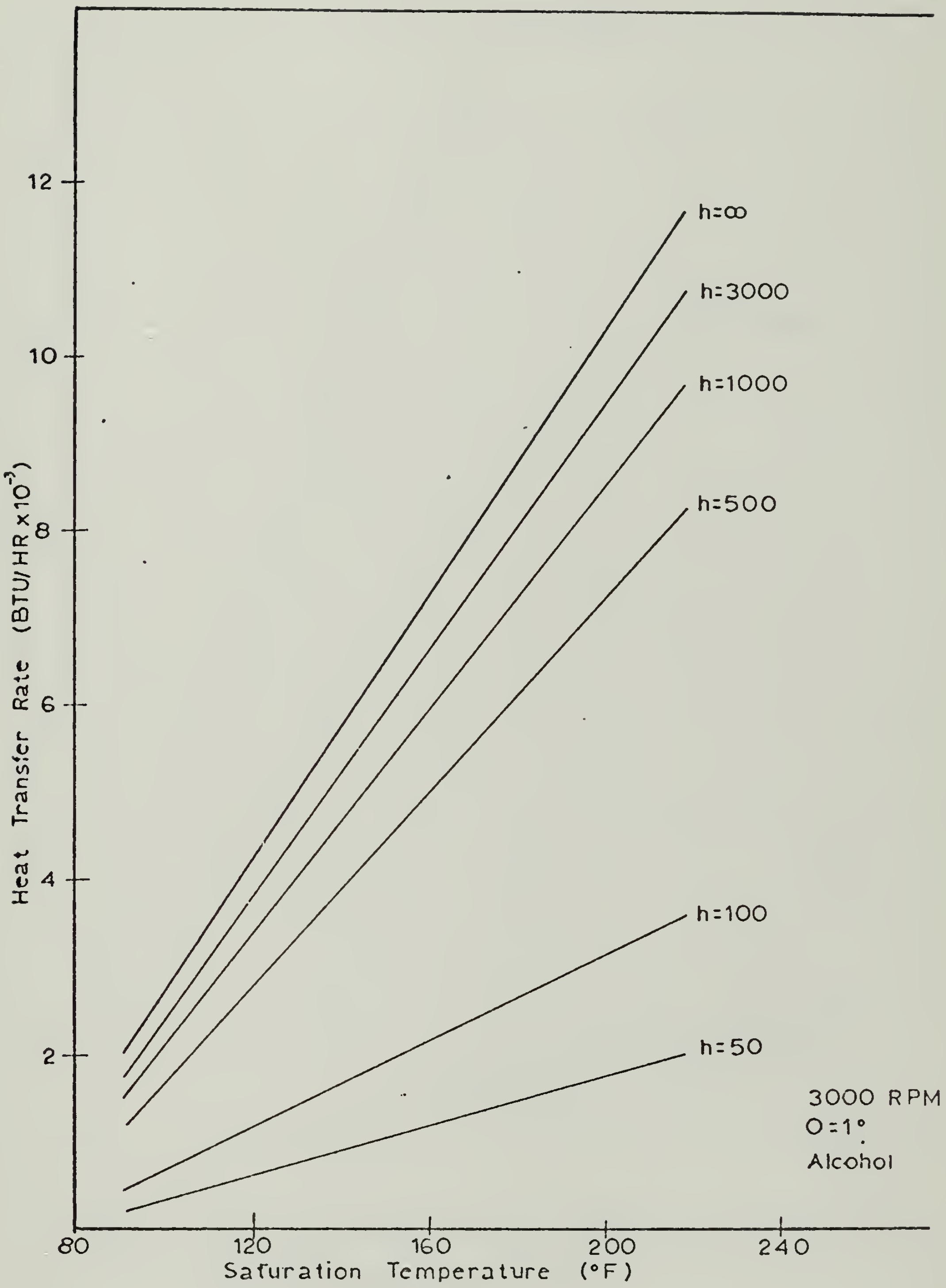

Fig. 8 Heat Pipe Response vs. Saturation Temperature for Alcohol at various external Heat Transfer Coefficients

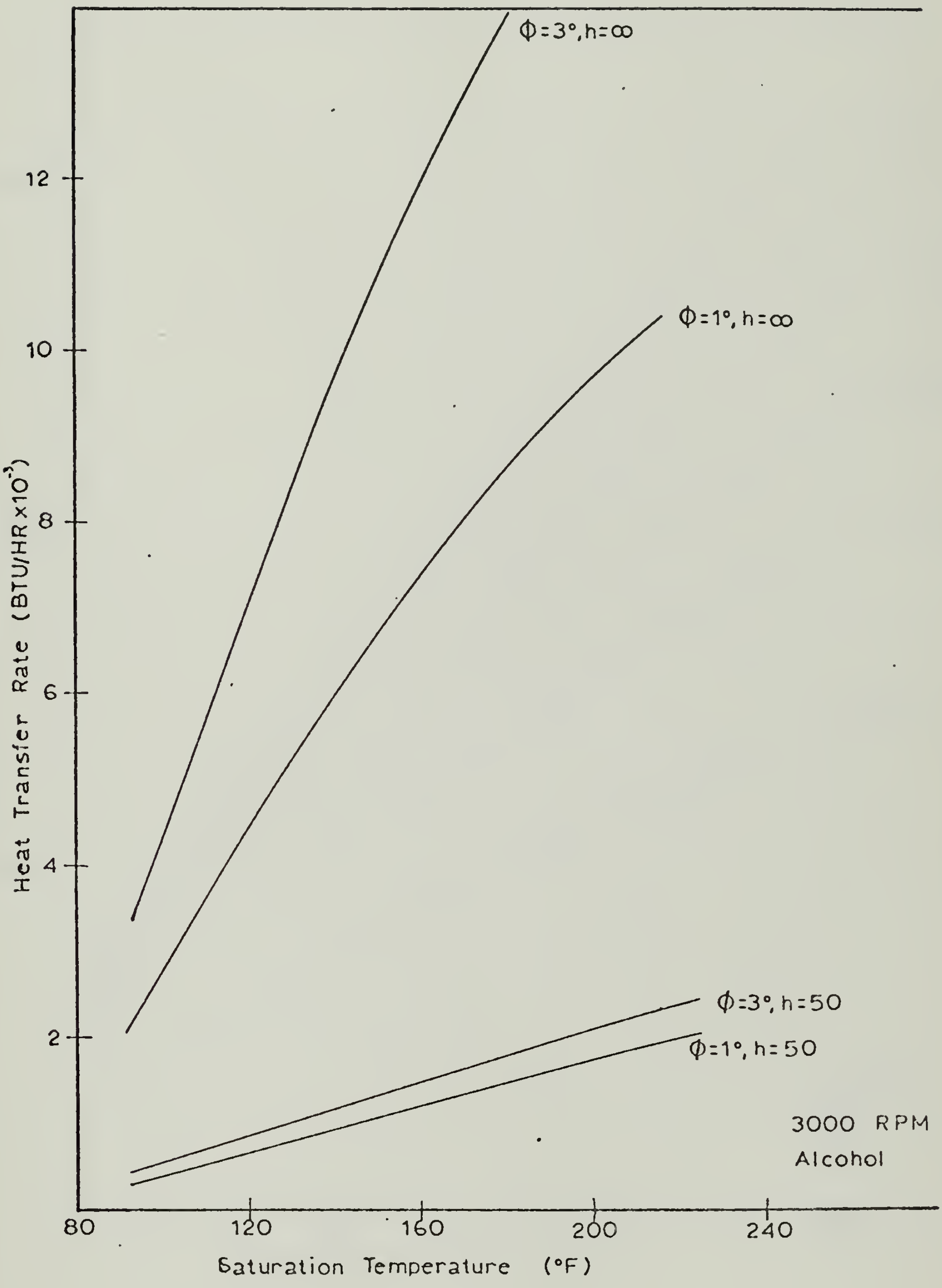

Fig. 9 Heat Pipe Response vs. Saturation Temperature for Alcohol at two Half Cone Angles and two exterior Heat Transfer Coefficients

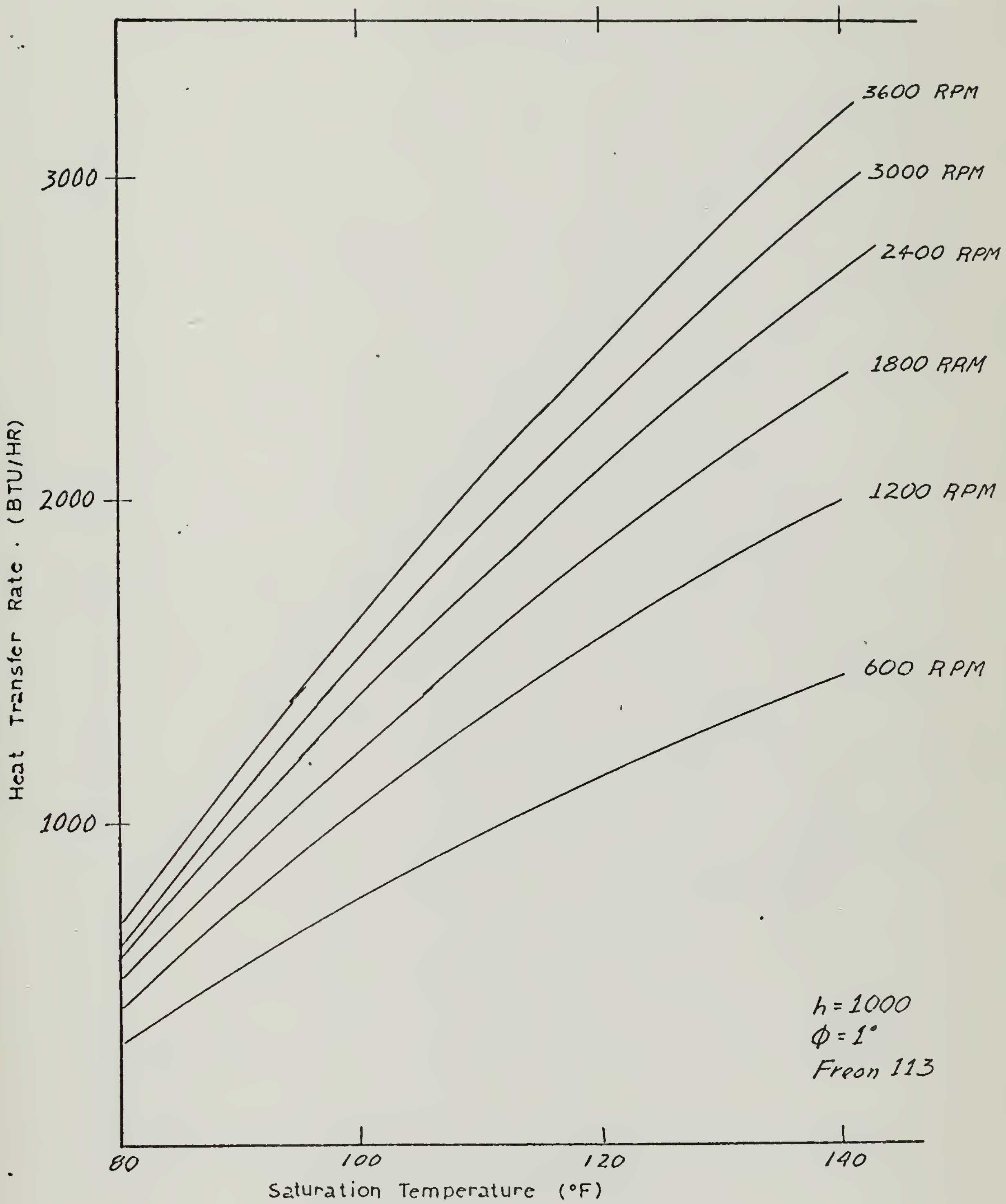

Fig. 10 Heat Pipe Response vs Saturation Temperature for Freon 113 at various Rotating Speeds

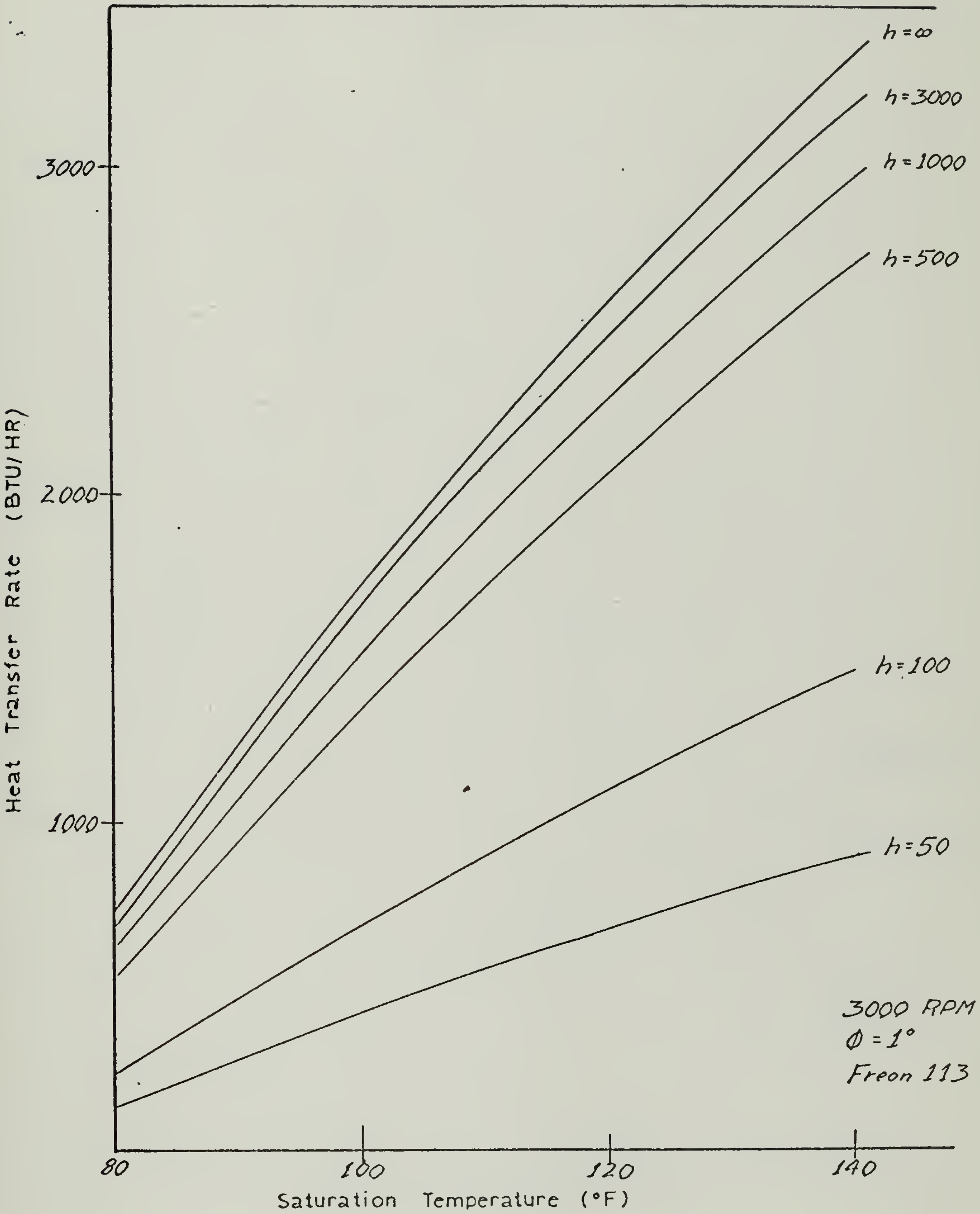

Fig. 11 Heat Pipe Response vs. Saturation Temperature for Freon 113 at various external Heat Transfer Coefficients

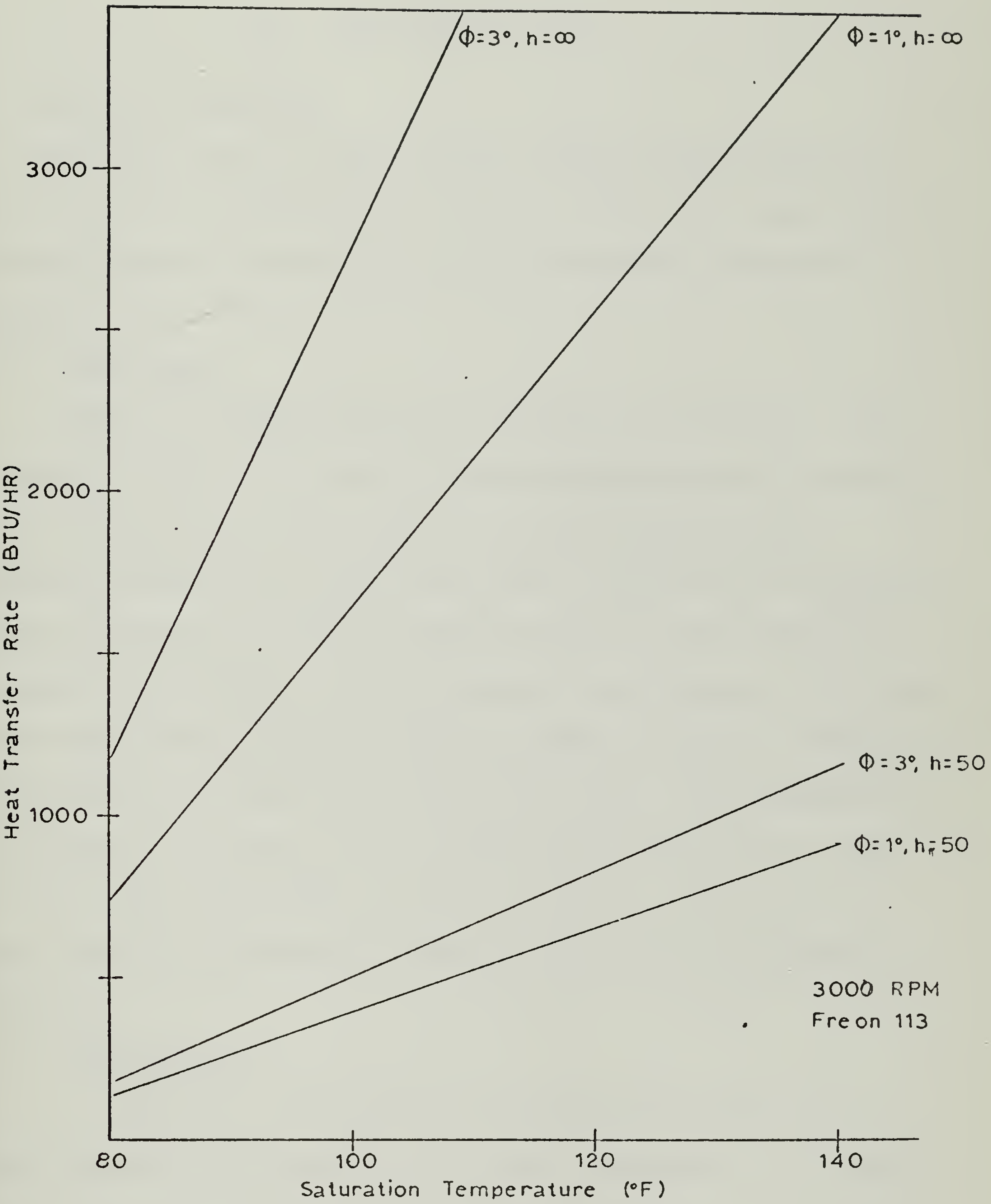

Fig. 12 Heat Pipe Response vs. Saturation Temperature for Freon 113 at two Half Cone Angles and two exterior Heat Transfer Coefficients

III. EXPERIMENTAL PROGRAM

A. DESCRIPTION OF EQUIPMENT

The equipment used to support the experimenatl program (Figures 14 and 15) was the same equipment used by Newton [ref. 5] with changes made as described below in order to increase instrumentation accuracy and performance reliability.

1. Power Supply

Power is furnished to the heater coils by a 120 volt d.c. motor generator set with an automatically regulated voltage output. The heater coils are connected in series with five load banks which consist of forty-eight 100 ohm resistances in each bank, each having the capability of being switched into parallel connection with the other resistors in the bank, thus providing a variable resistance from 33 ohms to 0.417 ohms. This variable resistance when connected in series with the 1.7 ohm heater coils provides power control from .433 kw to 7.6 kw. It is possible with this equipment to reproduce various heating loads within about 1%. The stability of the power supply precludes over-voltages which can cause serious damage to the equipment, leading to long periods of equipment inactivity.

2. Instrumentation

a. Temperature measurements are obtained from eight grounded copper-constantan thermocouples and two quartz thermometers. The thermocouples are used to measure a representative temperature of the evaporator wall, the vapor saturation temperature in the evaporator, and the exterior wall surface temperature of the condenser. The major differences from the

previous arrangements are in the condenser wall surface temperature and the cooling water effluent temperature measurements. A technique for implacing surface thermocouples was found in Ref. 1 and modified to fit this experiment. This technique is fully described in Appendix C, and consists of welding the copper-constantan junction and the junction itself to the condenser surface simultaneously in a Nitrogen atmosphere with spot welding equipment. Four thermocouples were welded to the condenser exterior surface with this technique. Each thermocouple was approximately evenly spaced longitudinally along the condenser.

The cooling water collector was modified in such a way as to insure mixing of the effluent and submergence of the quartz thermometer probe in the mixed water. This was done in order to eliminate large fluctuations in the temperature difference of the cooling water measured by the quartz thermometers.

b. Rotational speed measurement of the heat pipe is made by two means. A Systron Donner Counter 1013 Series measures the RPM using a magnetic pickup, and an electronic strobe is used as a check.

3. Auxiliary Equipment

In addition to the auxiliary equipment described in Ref. 5, a filling device (Figure 16) was constructed to improve the means of filling the heat pipe with the working fluid.

A drawing of the fill equipment is shown in Figure 16. The equipment consists of 1) a closed tube mercury manometer, 2) a graduated 250 ml reservoir, and 3) stopcocks and connections necessary to attach the equipment to the heat pipe and a vacuum pump.

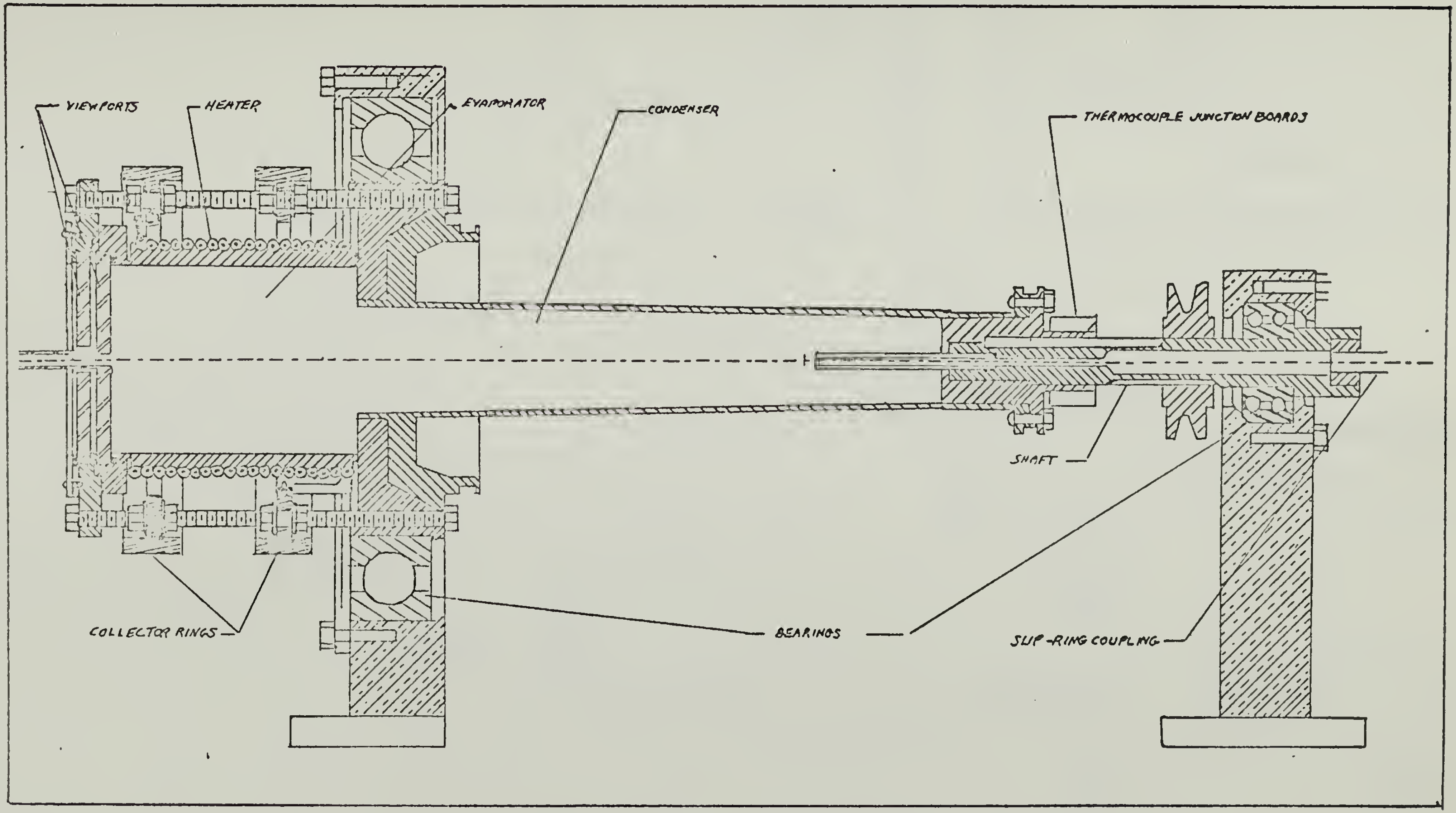

Fig. 14 Cross section of Experimental Heat Pipe

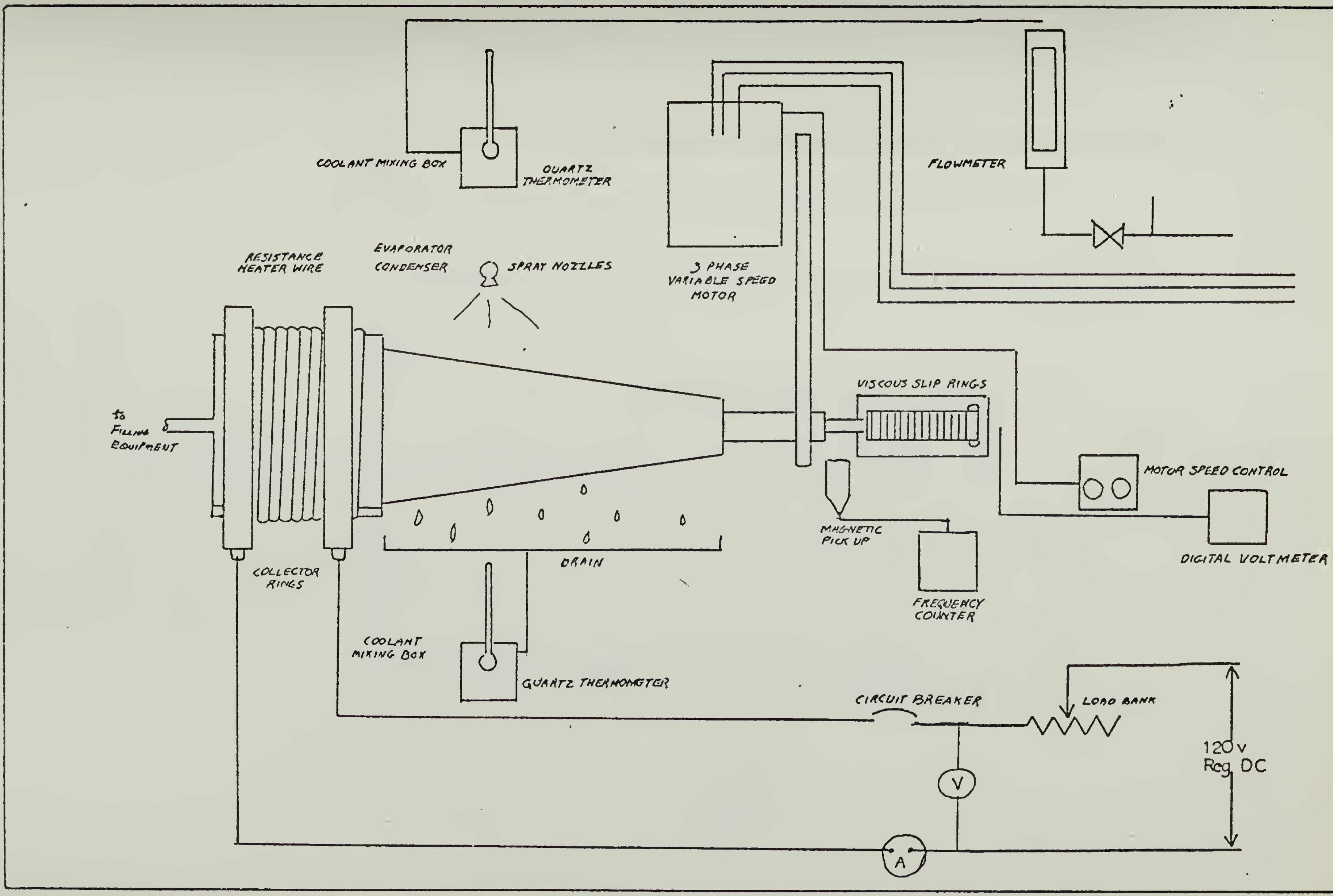

Fig. 15 Schematic of experimental equipment

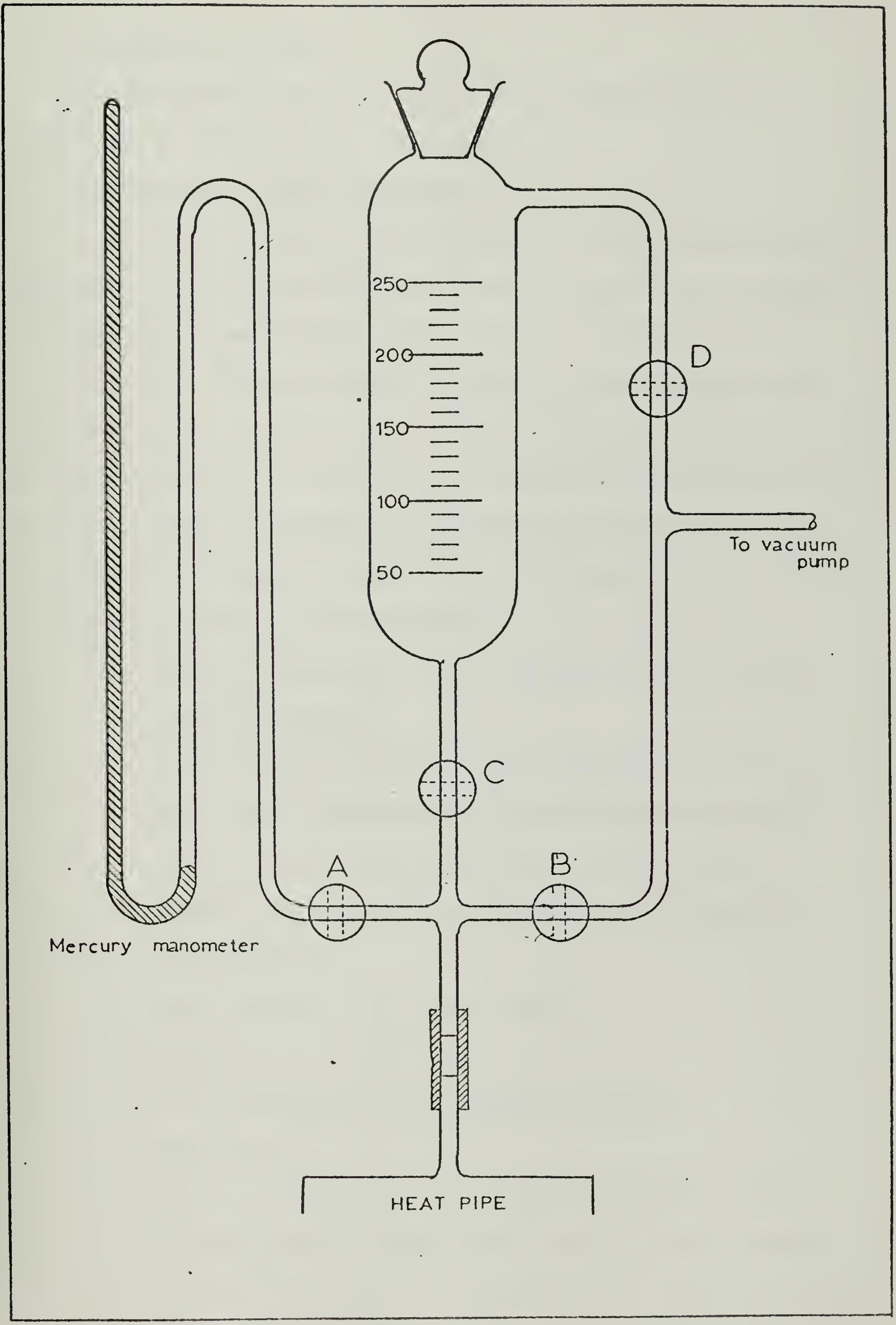

Fig. 16 Filling Apparatus

B. EXPERIMENTAL PROCEDURES

The experimental procedures consist of 1) cleaning and filling procedures, and 2) operational procedures.

1. Cleaning and Filling Procedures

In order to obtain film condensation in the heat pipe condenser when water is the working lfuid, the interior surface must be prepared to insure that proper "wetting" takes place. In addition to wetting, it is desirable to remove as much as possible of the non-condensible gases which may be present, and to fill the heat pipe with the same amount of fluid each time. The above goals are accomplished by performing the following. Note: Throughout this procedure, until step i. is begun, do not allow the heat pipe to remain empty. If necessary, fill with water until ready to accomplish the next step.

a. Place the heat pipe in the vertical position and mount the fill equipment.

b. With end windows and "O" rings removed, fill the heat pipe with a chlorinated hydrocarbon degreasing compound such as CCl_4 or Trichlorethylene. (Caution must be observed to avoid prolonged inhalation of the vapors of these compounds.)

c. Drain and fill with distilled water.

d. Repeat steps b. and c.

e. Fill the heat pipe three times with alcohol.

f. Repeat step c.

g. Fill the heat pipe with the following mixture: 8 parts distilled water, 2 parts ethyl alcohol, 2 parts 50% NaOH solution and 1/2 part 30% H_2O_2 solution. Warm the solution to approximately 140°F.

h. Rinse with distilled water until any suitable pH indicator reads about 7.0 pH. While refilling the heatpipe with water, watch the sides of the pipe carefully for signs of non-wetting. If these signs appear, repeat step g. and this step until pH of the rinse water is about 7.0 and the pipe (condenser) wall wets consistently.

i. When ready to fill, prepare the end windows for installation, drain the heat pipe, install the end windows with the appropriate "O" ring, gaskets, and bolt ring. Torque the bolts to 30 lb-in.

j. Immediately connect the fill equipment and start the vacuum pump.

k. Operate the fill equipment as follows. Start with all stopcocks shut.

   (1) Open stopcock "A".

   (2) Slowly open stopcock "B".

   (3) Pump until minimum absolute pressure is reached (about 5 mm Hg or less) approximately 1/2 hour.

   (4) Shut stopcock "B".

   (5) Vent and fill the graduated flask with working fluid to desired level.

   (6) After the flask stopper is in place, slowly open stopcock "D", allow the fluid to boil about 1 minute to degas.

   (7) Shut stopcock "D", slowly open stopcock "C" and allow the desired amount of fluid to enter the heat pipe.

(8) Record the pressure and output from thermocouple channel no. 5.

(9) Seal the fill tube with heat.

2. Operational Procedure

Having completed the filling procedure, the heat pipe is ready to run at a pre-determined RPM. About 10 drops of lubricating oil are added to the oil fill tube at the top of the large block. The cooling water lines are turned on so that the rotameter is at approximately 30% flow.

The drive motor is turned on and the heat pipe is slowly brought up to the desired RPM. Once a liquid annulus has formed in the evaporator and the desired RPM has been reached, the DC motor generator is turned on and power is added to the evaporator. Having reached thermal equilibrium for a particular power setting, data was taken by the instrumentation described earlier.

Shut-down is accomplished by first shutting off the current to the heater, and then decreasing the RPM by use of the remote control unit.

Cooling water flow rate and temperature difference data is then reduced by the equation

$$Q = \dot{m}\, c_p \Delta T$$

to determine the experimental heat transfer rate of the heat pipe. Condenser exterior wall temperature data is then used in the analytical solution for the same conditions.

C. EXPERIMENTAL RESULTS

1. Preliminary Results

Using de-ionized, distilled water as the working fluid, the heat pipe was rotated at the various RPMs. A preliminary energy balance made on the cooling water flow through the condenser cooling box compared to the electrical power input indicated that up to 10% of the heat added to the heating coils of the evaporator was not recovered in the condenser, suggesting unmeasurable heat losses from the system by mechanisms other than through the heat pipe and into the cooling system. The probable mechanisms are losses to ambient from the evaporator heater coils, and losses to the main bearing cooling water. Further insulation of the system, however, appears at this time to be unfeasible.

Limitations were placed on operating the heat pipe above 8 Kw due to the temperature in the heating coils developed at that power level as indicated by a red glow from the coils. Another limitation was the operating pressure within the heat pipe. These limitations precluded operation of the pipe at low RPM and high power levels.

2. Visual Observations

Using a strobe light, visual observations were made through the end window. Film condensation appeared to be taking place since the condenser surface was mirror smooth. Comparison with the appearance of the condenser during Newton's operation when noticeable waves and surface irregularities were evident support this conclusion. From these observations it was estimated that film condensation was taking place over greater than 90% of the condenser surface at all power levels and RPMs. A small portion of the remote end of the condenser did appear to undergo dropwise condensation, but this area became smaller as the power and RPM were increased.

3. Discussion of Experimental Results

The results obtained while operating the heat pipe are plotted in Figures 17, 18, and 19, together with solutions of the analytical model for the conditions achieved during operation, and the solutions to an analysis performed by Sparrow and Hartnett, [ref. 3], for condensation on a rotating cone. The Sparrow and Hartnett results are shown to indicate the state of the technology at the beginning of the original investigations of Ballback and to serve as a form of reference from which these analyses are improvements.

The heat pipe was operated successfully on three occasions, identified here in chronological order as Runs 1, 2, and 3. Runs 1 and 3 were performed in order to establish repeatability of conditions and data. Run 2 was performed in order to compare the effects of dropwise condensation with film condensation, and with Newton's dropwise data. Run 1 was made with the first use of the fill equipment. Due to uncertainties in procedure, lack of experience, and fear of losing condenser wetting if the pipe was permitted to dry, the heat pipe was evacuated for 10 minutes to a final pressure of 19 mm Hg before filling and sealing. Upon completion of Run 1 the pipe was wiped lightly with machine oil in an effort to promote dropwise condensation. Filling for Run 2 was accomplished in the same manner as Run 1. Run 2 was conducted and dropwise condensation was achieved. The cleaning procedure was then carried out and Run 3 was conducted. However, while evacuating the pipe prior to filling it, a significantly lower pressure could be attained. The pipe was filled and sealed after 30 minutes of evacuation, and at a pressure prior to filling of 4.5 mm Hg. Subsequent operation was successful in that film condensation was achieved, even though the heat pipe was dry prior to filling.

Four major areas of discussion were opened by the experimental program: (1) the results of efforts to reduce the previous experimental uncertainty, (2) the effects of film vs dropwise condensation on heat pipe response, (3) the effects of non-condensibles in the working fluid on the response of the pipe, and (4) the uncertainty in measurement of effective condenser length.

The experimental data indicated a significant reduction in experimental uncertainty. Newton was able to obtain an average uncertainty in the measurement of heat transfer rate of ±588 BTU/HR. The efforts of the present project succeeded in reducing the uncertainty in this measurement to less than ±50 BTU/HR. Additionally, the measurement of the exterior condenser surface temperature made it possible to eliminate the dependance of the analytical solution on the determination of the exterior heat transfer coefficient.

The efforts to achieve film condensation were also successful and were important in that the analytical solution is based on this condensation mechanism. Comparing the results of Run No. 2 with those of Runs Nos. 1 and 3 indicate this success. The increase in heat transfer with dropwise condensation is apparent. The flattening of the condensate drops with increasing RPM, with its resultant increase in centrifugal forces, reducing the non wetted area in the condenser and thereby reducing the heat transfer rate can be seen by comparing the data for the three different RPMs.

A comparison of the Run 2 results with Newton's experimental results are plotted in Figure 20. This comparison indicates that higher heat transfer rates were achieved during Run 2 for similar conditions. This supports the assumed improvement in ability to remove non-condensible

gases from the working fluid due to the modified filling techniques and equipment. Newton's analytical results, however, were below his experimental results, and on the order of 2500 BTU/HR less than the analytical results of this thesis. This difference in analytical results may be explained by the different means of taking into account the external heat transfer coefficient, due to the change in instrumentation described in Section II.A.2 of this paper.

The effects of non-condensible gases in the vapor space are not as readily apparent. Gebhart [ref. 4] indicates that a very small concentration of air in a water vapor significantly reduces the surface heat transfer coefficient in film condensation by effectively blanketing the film with the more dense air. This effect would be increased with decreasing temperature as the density ratio between the vapor and the air is reduced with decreasing temperature. An increase in the gravitational field would also tend to increase the blanketing effect by effectively increasing the difference in weights of the two gases, air and vapor. Both of these effects are supported by the data of Runs No. 1 and No. 3. The convergence of the data with increasing temperature and the divergence of the data with increasing RPM is significant. From this discussion it can be seen that the experimental results support the presence of non-condensible gases, specifically air, in the vapor space of the experimental model. This suggests a possible reason for the difference between the experimental results and the analytical curve.

The proximity of the data to the Sparrow and Hartnett results is misleading, since their results are limited to cones "which were not too slender" by the assumptions they made in order to arrive at a similarity solution. These results are plotted here only to indicate the state of

the art at the beginning of the initial analysis by Ballback, and to show the changes that arise from including interfacial shear, small cone angles, and the vapor pressure gradient in the analysis.

Finally, the surface temperature measurements from Runs 1 and 3 indicate that the determination of effective condenser length may be in error. The raw data plotted for a representative data point in Figure 21 indicates that a longitudinal temperature gradient existed on the condenser surface, with a marked increase in temperature toward the evaporator section of the heat pipe. This gradient was much less in Run No. 3 when it was known that the concentration of air in the vapor space was reduced by improved filling techniques. This suggests that the effective length varies inversely with concentration of non-condensible gases in the vapor, due to the tendency of the non-condensible gases to flow toward the evaporator because of their greater relative mass. Therefore, the effective condenser length used in the theoretical calculations may be too large. A shorter condenser length in the analytical calcuations would reduce the results of both this thesis and those of Sparrow and Hartnett without changing the experimental results.

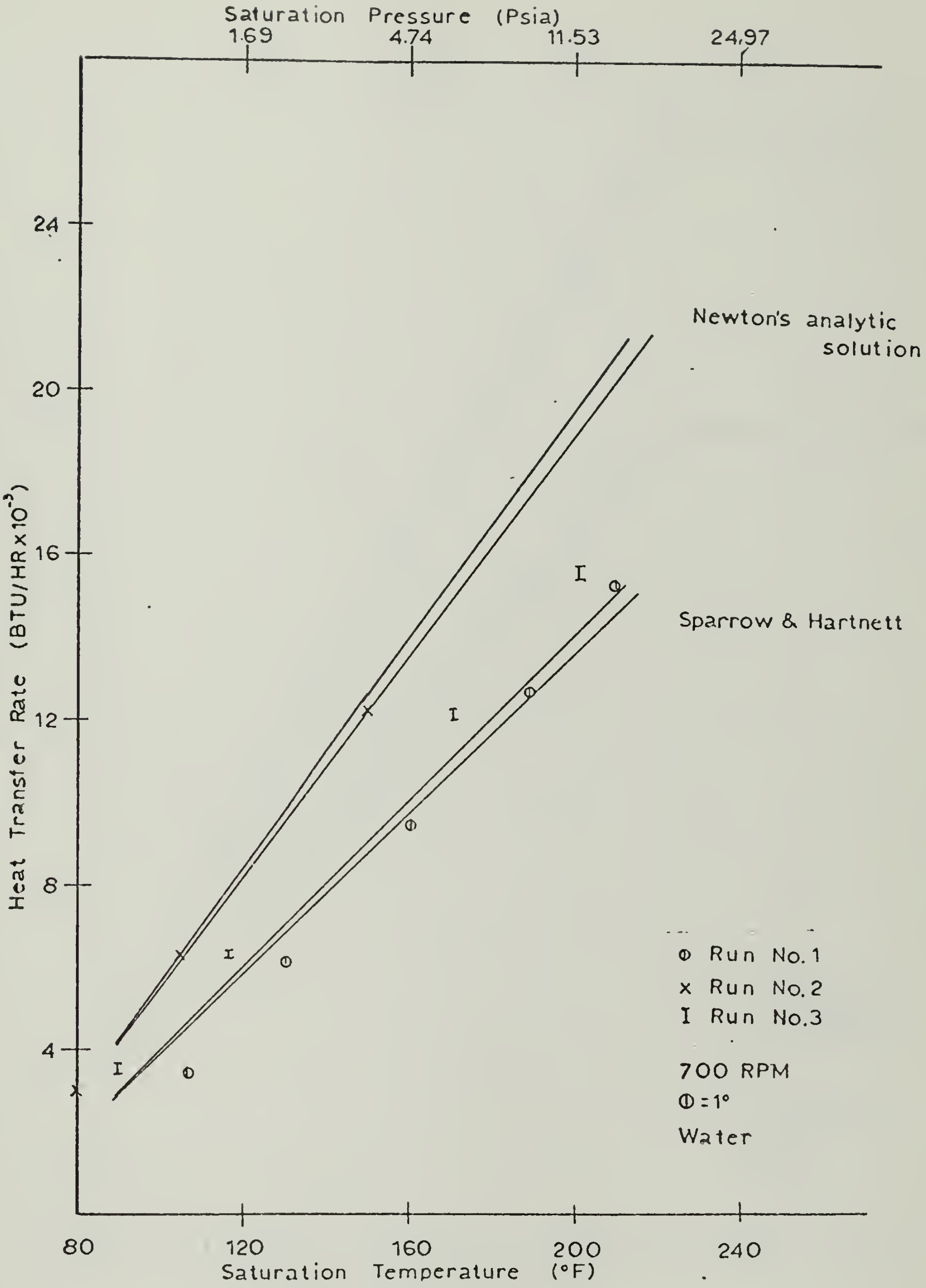

Fig. 17 Heat Pipe Response vs. Saturation Temperature, Experimental Heat Pipe operating with Water at 700 RPM

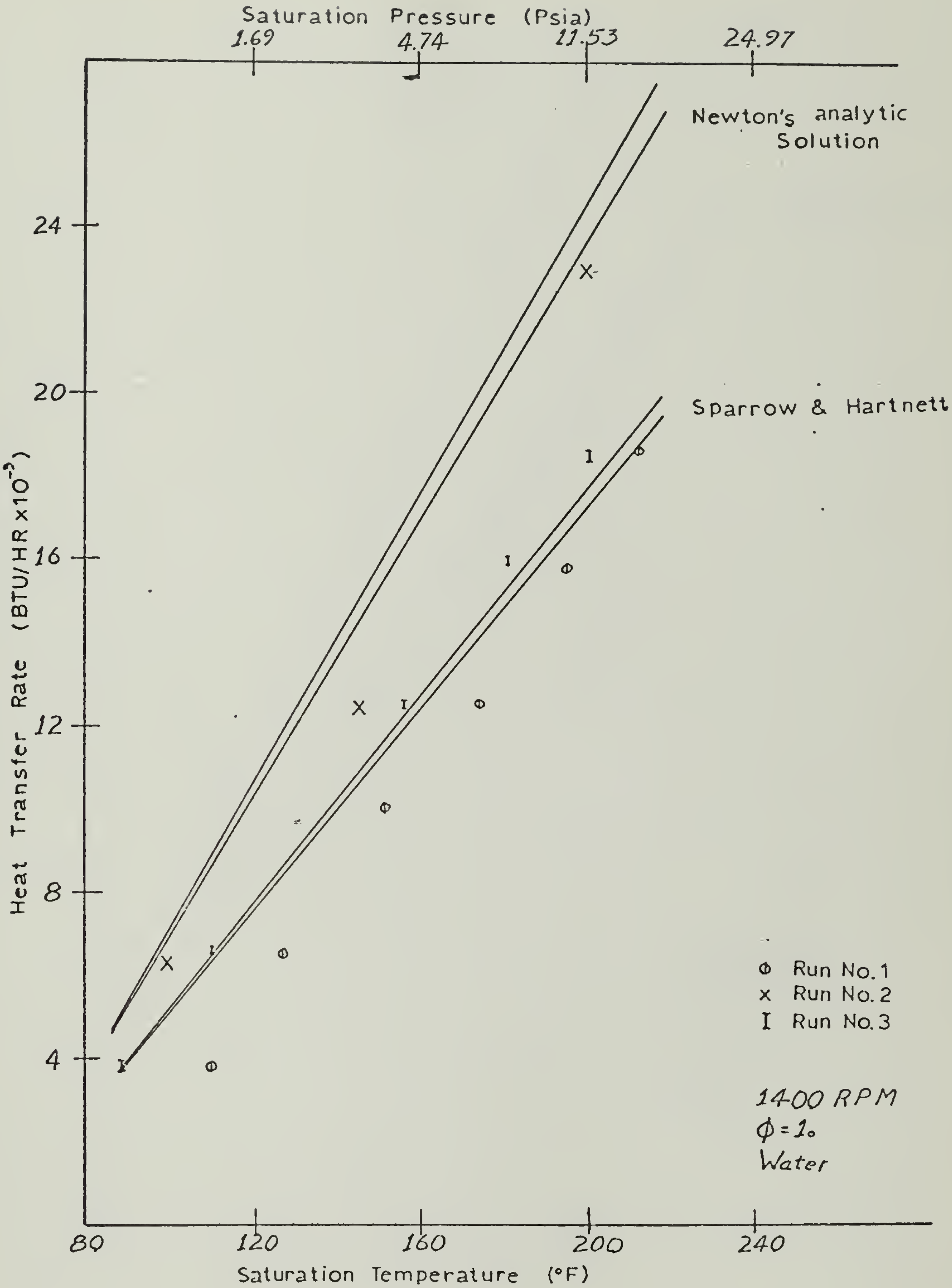

Fig. 18 Heat Pipe Response vs. Saturation Temperature, Experimental Heat Pipe operating with Water at 1400 RPM

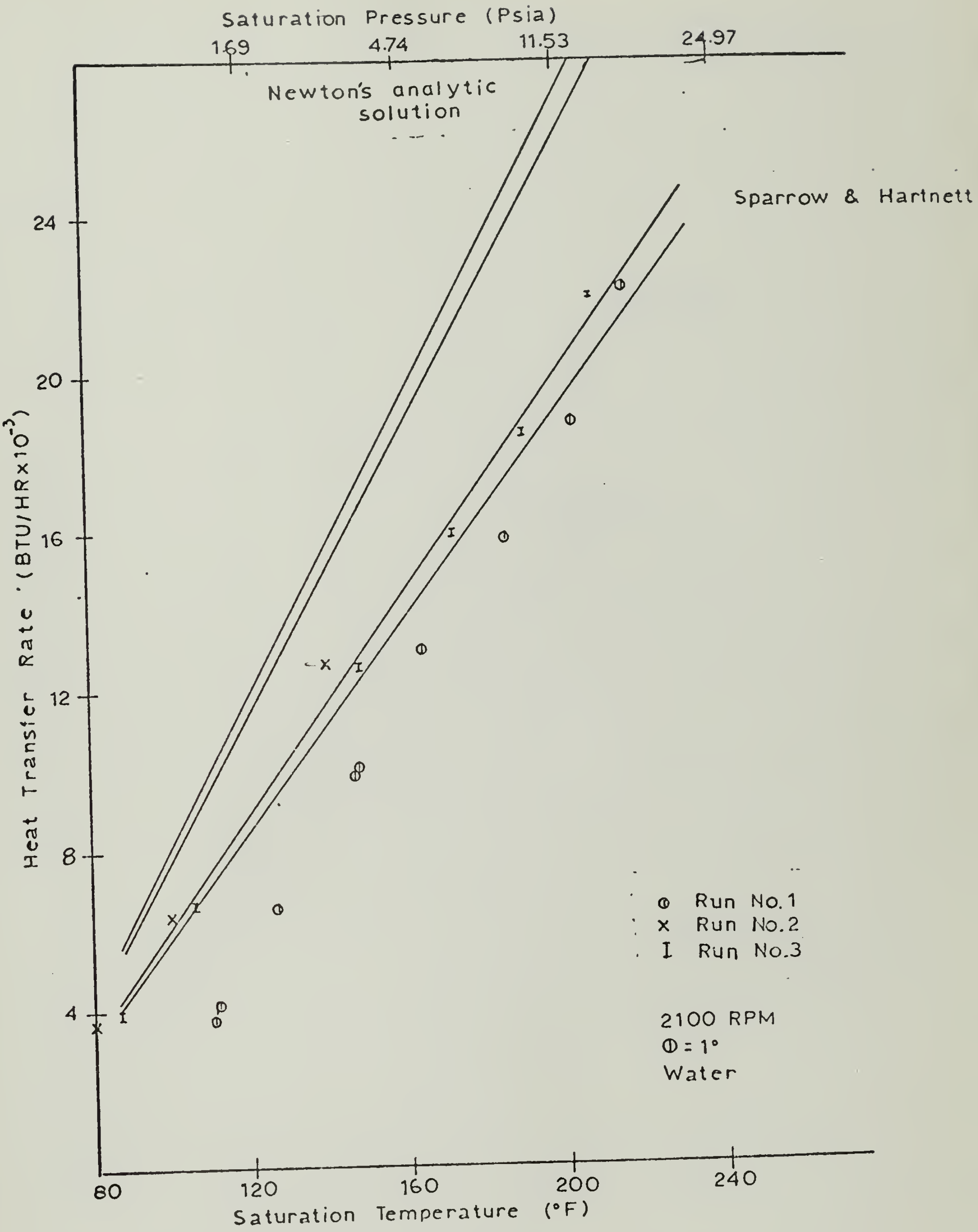

Fig. 19 Heat Pipe Response vs. Saturation Temperature, Experimental Heat Pipe operating with Water at 2100 RPM

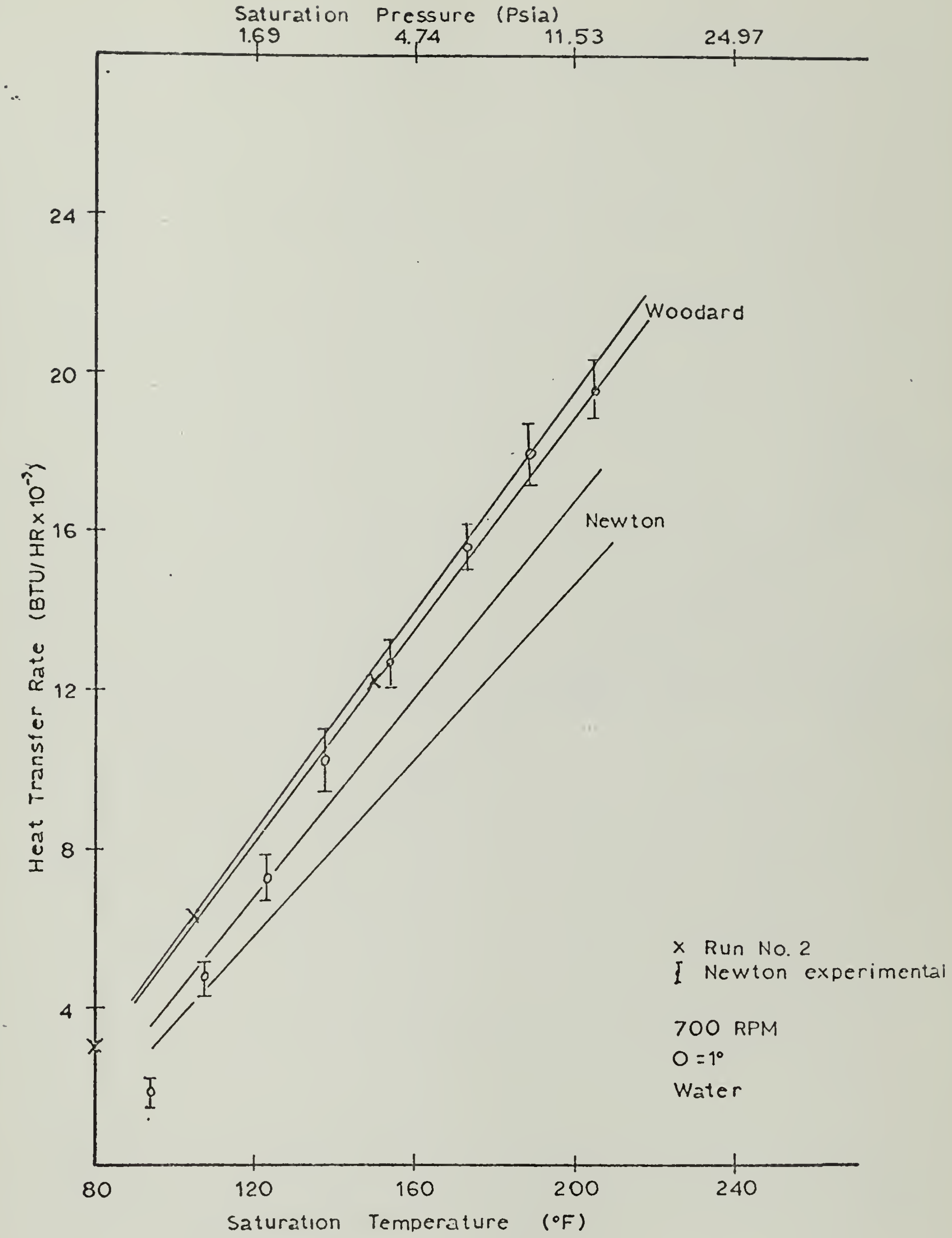

Fig. 20 Heat Pipe Response vs. Saturation Temperature

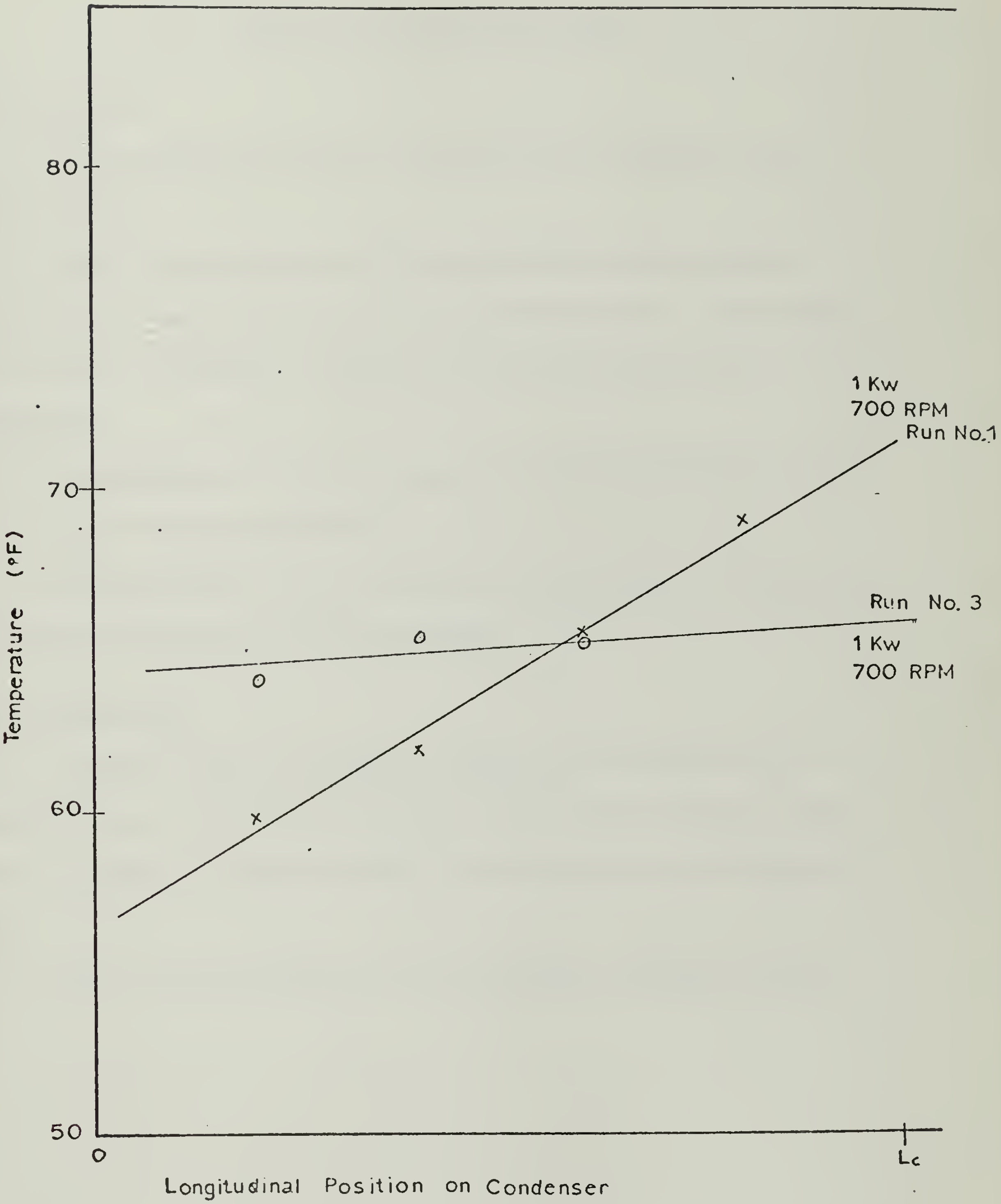

Fig. 21 Condenser Surface Temperature vs. Longitudinal Position on Condenser Exterior Surface

IV. CONCLUSIONS AND RECOMMENDATIONS

A. CONCLUSIONS

1. The rotating non-capillary heat pipe is an effective heat transfer device.

2. Smooth film condensation was achieved during experimental operation when desired and its effects were significant. Heat transfer rate with film condensation was less than that with drop wise condensation.

3. The performance of the heat pipe is strongly influenced by the exterior heat transfer coefficient.

4. The performance of the heat pipe is degraded by the presence of non-condensible gases in the working fluid.

B. RECOMMENDATIONS

1. In order to make a systematic study of the effect of non-condensible gases, improve the evacuation and filling technique, and improve the method of determining the concentration of non-condensible gases.

2. Improve the determination of the effective condenser length.

APPENDIX A

CALIBRATION

1. Calibration of Thermocouples. The calibration of the condenser surface thermocouples which were manufactured in place, was accomplished by constructing an enclosure of thermal insulation around the heat pipe, and providing a source of steam to the enclosure directed to the condenser box and the interior of the heat pipe. The quartz thermometers were suspended in the condenser box as temperature references. Agreement between the previously calibrated quartz thermometers, the installed thermocouples and previously more extensively calibrated thermocouples of the same material but unattached to the pipe, at the steam point was reached. It was determined that the in-place thermocouples deviated less than 1.0°F from the earlier calibration curve.

2. Calibration of the Rotameter. The method used in the calibration of the cooling water flow rotameter consisted basically of using a Toledo scale to measure the mass of the coolant flowing into a large receptical placed on the scale. As coolant flowed into the container, an arbitrary starting point on the scale was established and the stop watch was started. When the weight on the scale increased by 40 pounds the stop watch was stopped and the time recorded. This procedure was repeated several times at each flow rate and data for 10, 20, 30, 40 and 50% full rotameter scale flow rates were recorded. (This was done in order to insure that flow through the system was constant and duplicated the experimental conditions while still providing reliable calibration data.)

(See figure below.) A valve and tee piping arrangement was attached to the outlet of the rubber hose which was normally attached to the condenser cooling box, supplying water to the spray nozzles.

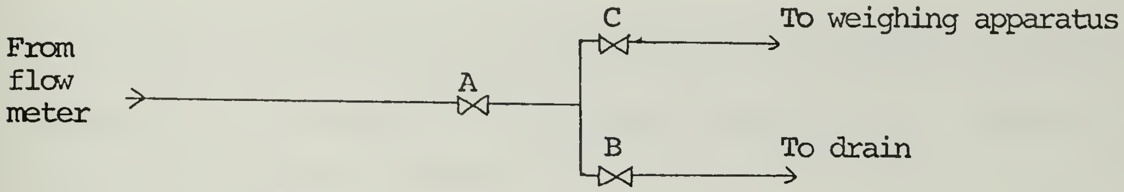

By establishing the desired flow with valve A while valve B was open, then closing valve B and opening valve C, it was possible to control the flow rate and back pressure of the system while calibrating the rotameter. This arrangement provided consistant repeatable measurements of the flow rate, which could be correlated to the readings on the rotameter. The data was plotted and a straight line was drawn through the data. The equation for that line was determined to provide flow measurement accuracy with the rotameter within 1% of the flow rate through the system, measured by the calibration equipment.

APPENDIX B

TECHNIQUE FOR WELDING SURFACE TEMPERATURE MEASURING THERMOCOUPLES

A means of determining the temperature of the condenser surface was determined to be necessary. The technique described here, adapted from ref. 1, was used with success.

The exterior kapton insulation of the thermocouple leads was stripped back 1/2", 1/8" of insulation was then removed from the individual copper and constantan wires. The stainless steel surface was prepared by cleaning with fine emery cloth and acetone. The wire was taped in place to insure no movement during the welding process. The constantan wire was oriented over the spot where the temperature measurement was desired and the copper lead arranged above it. The spot welding probe, after the tip had been filed clean, was arranged directly above the crossing point of the two wires and depressed with a force of approximately two lbs. The energy source, a Unitek 1065 Weldmatic, was set at 5 watt seconds. It is important that good contact is established between the stainless steel surface, the constantan, the copper and the welding probe. Grounding of the welding machine to the base metal is accomplished insuring that the ground path does not include bearing surface. With all preparations made, the current is applied. If the weld is not acceptable, it is necessary to begin again with the preparation of the thermocouple wire. Figure 22 shows the arrangement of the equipment and material. The inset shows the desired appearance of the completed thermocouple junction.

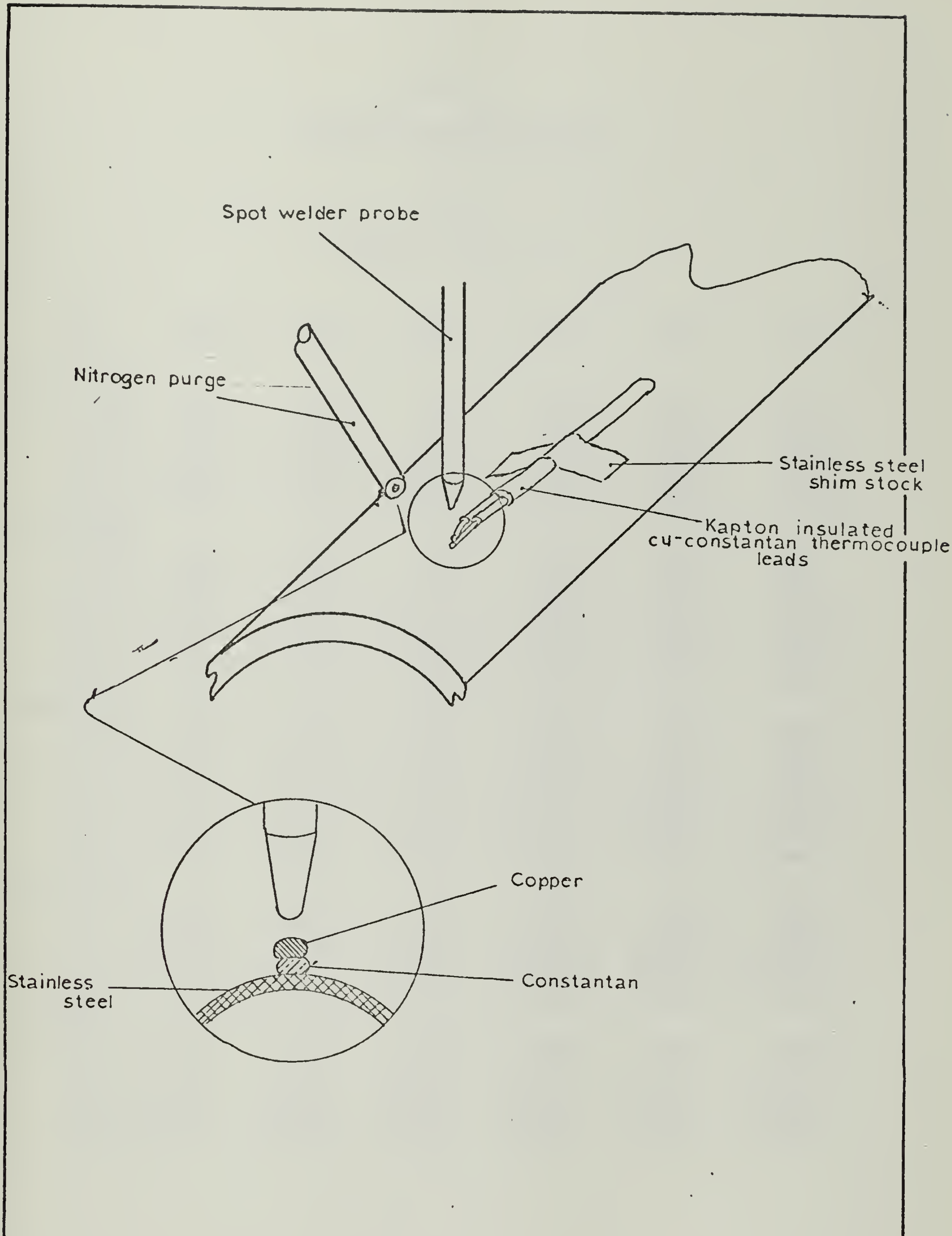

Fig. 22 Thermocouple Welding Technique

APPENDIX C

TABULATED ANALYTICAL DATA

Water

Half Cone Angle = 1°

RPM T_s	600	1200	1800	2400	3000	3600
H = 50.0						
98.4	426.3	430.6	437.3	433.3	433.9	434.4
115.3	678.4	685.7	688.8	690.5	691.6	692.4
141.8	1073.4	1085.8	1090.9	1093.8	1095.7	1097.1
174.3	1558.0	1576.6	1584.2	1588.5	1591.4	1593.4
205.6	2025.4	2049.4	2060.0	2065.7	2069.5	2072.2
H = 100.0						
98.4	799.3	817.8	825.6	829.2	833.1	835.7
115.3	1267.9	1299.4	1313.3	1320.8	1325.1	1329.6
141.8	2001.1	2055.7	2077.6	2090.2	2099.9	2105.4
174.3	2902.7	2982.4	3015.3	3035.3	3048.5	3057.7
205.6	3771.9	3876.8	3921.4	3947.2	3764.7	3976.9
224.3	4297.2	4411.3	4461.8	4490.6	4510.5	4523.7
H = 500.0						
98.4	2488.3	2769.7	2905.5	2989.9	3046.4	3090.7
115.3	3876.5	4341.6	4569.4	4710.2	4809.1	4882.8
141.8	6040.7	6798.8	7173.7	7406.5	7569.6	7691.1
174.3	8701.3	9819.2	10371.5	10717.4	10959.9	11140.8
205.6	11269.6	12744.5	13477.2	13934.1	14255.9	14495.5
224.3	13529.9	14720.1	15426.8	15900.2	16242.7	16504.3
H = 1000.0						
98.4	3270.0	3844.6	4145.4	4339.7	4478.7	4584.6
115.3	5019.6	5962.6	6461.0	6784.9	7017.9	7195.8
141.8	7758.0	9274.1	10082.9	10611.4	10992.9	11285.3
174.3	11164.8	13365.0	14547.3	15323.1	15884.6	16315.9
205.6	14499.8	17359.2	18906.4	19925.7	20665.3	21234.5
H = 10^{15}						
98.4	4623.2	6044.5	6938.9	7589.1	8095.6	8510.2
115.3	6936.3	9166.7	10584.0	11621.1	12434.6	13100.6
141.8	10584.3	14065.3	16295.5	17936.4	19229.3	20291.5
174.3	15198.5	20187.2	23399.3	25771.4	27645.7	29189.0
205.6	19776.2	26229.4	30407.7	33505.7	35961.3	37988.4

Water

Half Cone Angle = 3°

RPM T_s	600	1200	1800	2400	3000	3600
H = 50.0						
98.4	513.9	517.3	518.6	519.4	519.9	520.3
115.3	818.6	824.3	826.7	828.0	828.9	829.5
141.8	1296.1	1305.8	1309.8	1312.0	1313.5	1314.6
174.3	1881.9	1896.5	1902.4	1905.7	1908.0	1909.5
205.6	2446.9	2466.2	2474.0	2478.5	2481.4	2483.5
H = 100						
98.4	975.6	990.4	996.6	1000.1	1002.4	1004.0
115.3	1550.6	1576.3	1587.0	1593.1	1597.1	1599.9
141.8	2451.7	2494.9	2512.8	2523.1	2529.8	2534.7
174.3	3557.2	3621.8	3648.6	3663.9	3674.1	3681.4
205.6	4624.8	4710.2	4745.8	4766.1	4779.6	4789.2
H = 500						
98.4	3295.4	3559.5	3681.7	3755.2	3805.4	3842.2
115.3	5165.2	5609.0	5816.4	5941.9	6027.7	6090.9
141.8	8087.6	8817.3	9160.9	9369.5	9512.5	9618.1
174.3	11678.9	12758.3	13268.5	13578.8	13791.8	13949.2
205.6	15161.4	16588.5	17264.3	17675.9	17958.7	18167.7
H = 1000						
98.4	4581.2	5165.4	5457.7	5641.2	5769.9	5866.3
115.3	7117.6	8079.8	8567.4	8875.7	9093.0	9256.5
141.8	11076.9	12637.7	13435.9	13943.3	14302.1	14572.9
174.3	15948.2	18242.1	19420.6	20171.7	20703.9	21106.0
205.6	20678.0	23705.0	25265.0	26261.1	26967.9	27502.4
H = 10^{15}						
98.4	7236.1	9031.1	10112.4	10874.3	11454.6	11918.2
115.3	11037.1	13865.1	15590.2	16816.1	17755.9	18510.5
141.8	16962.4	21415.2	24156.6	26116.9	27627.1	28844.4
174.3	24276.9	30727.8	34718.0	37580.9	39791.5	41577.2
205.6	31375.2					

Alcohol

Half Cone Angle = 1°

RPM T_s	600	1200	1800	2400	3000	3600
H = 50						
86	213.8	224.6	229.4	232.2	234.1	235.4
122	662.4	706.3	726.3	738.2	746.2	752.1
158	1097.5	1177.9	1214.8	1236.9	1352.0	1263.0
194	1515.9	1636.6	1692.7	7726.5	1749.5	1766.5
H = 100						
86	354.1	389.9	407.2	417.8	425.1	430.5
122	1053.7	1187.1	1254.1	1296.3	1325.8	1348.0
158	1718.2	1953.2	2073.3	2149.5	2203.4	2244.1
194	2339.2	2680.6	2857.7	2971.2	3052.0	3113.1
H = 500						
86	693.8	875.8	988.8	1070.1	1133.1	1184.0
122	1876.2	2418.7	2768.4	3026.7	3230.7	3398.6
158	2957.6	3839.3	4415.1	4844.4	5186.0	5468.7
194	3913.9	5108.8	5898.0	6491.1	6966.0	7361.2
H = 1000						
86	779.2	1020.9	1181.7	1303.3	1401.0	1482.7
122	2060.1	2743.2	3210.4	3570.7	3865.3	4114.8
158	3224.1	4314.9	5068.0	5652.8	6133.7	6543.1
194	4242.0	5699.0	6713.0	7505.3	8160.1	8719.8
H = 3000						
86	846.3	1142.4	1350.5	1514.3	1650.5	1767.4
122	2199.1	3002.5	3577.3	4035.9	4421.6	4756.3
158	3423.0	4689.1	5600.3	6331.0	6947.9	7485.0
194	4484.4	6157.5	7368.3	8343.1	9168.9	9890.1
H = 10^{15}						
86	883.1	1212.3	1450.7	1642.8	1805.5	1947.6
122	2273.0	3146.5	3786.7	4307.3	4752.1	5143.5
158	3527.6	4894.4	5900.5	6721.3	7424.5	8044.8
194	4610.6	6406.7	7733.8	8819.7	9752.3	10576.7

Alcohol

Half Cone Angle = 3°

RPM T_s	600	1200	1800	2400	3000	3600
H = 50						
86	267.7	276.9	280.9	283.2	284.7	285.8
122	840.6	819.5	896.5	906.5	913.2	918.0
158	1402.9	1474.4	1506.1	1524.6	1537.1	1546.2
194	1948.7	2057.6	2106.2	2134.8	2154.1	2168.2
H = 100						
86	463.9	497.6	513.1	522.3	528.6	533.3
122	1408.2	1540.6	1603.6	1642.0	1668.5	1688.1
158	2320.5	2557.3	2671.7	2742.0	2790.6	2826.7
194	3183.2	3533.7	3705.3	3811.6	3885.5	3940.5
H = 500						
86	1034.4	1266.3	1402.6	1497.0	1568.0	1624.1
122	2841.8	3563.5	4006.8	4323.3	4566.6	4762.5
158	4528.7	5722.4	6466.3	7002.7	7418.3	7754.9
194	6022.7	7663.2	8699.4	9453.3	10041.8	10521.2
H = 1000						
86	1203.0	1538.0	1751.5	1907.9	2030.5	2130.9
122	3214.7	4190.3	4834.3	5318.0	5705.1	6027.1
158	5080.0	6661.1	7716.4	8515.4	9159.0	9697.2
194	6785.8	8839.5	10278.1	11375.4	12264.6	13012.0
H = 3000						
86	1343.5	1782.4	2082.0	2312.6	2500.8	2660.0
122	3511.2	4722.9	5570.0	6234.0	6784.2	7255.5
158	5512.2	7444.9	8806.2.	9879.5	10772.9	11541.4
194	7234.7	9806.5	11630.5	13076.1	14284.8	15328.4
H = 10^{15}						
86	1424.0	1930.6	2290.1	2575.1	2813.5	3019.5
122	3675.4	5032.3	6011.7	6798.5	7468.7	8043.8
158	5749.2	7894.6	9451.3	10707.0	11772.5	12704.3
194	7521.9	10355.1	12420.9	14093.6	15517.5	16766.2

Freon

Half Cone Angle = 1 °

RPM T_s	600	1200	1800	2400	3000	3600
H = 50						
80	120.1	130.3	135.1	138.0	140.0	141.4
100	331.5	367.8	385.6	396.7	404.3	410.0
120	527.7	592.4	624.8	645.2	659.4	670.1
140	713.9	808.3	856.2	886.5	907.9	924.0
H = 100						
80	183.3	211.2	225.9	235.4	242.2	247.3
100	480.4	569.1	618.2	65019	674.8	693.3
120	746.2	895.5	980.1	1037.3	1079.6	1112.6
140	992.8	1201.9	1323.3	1404.7	1465.9	1514.0
H = 500						
80	300.6	393.2	454.8	501.4	538.9	570.2
100	720.5	958.3	1121.4	1247.4	1350.6	1438.0
120	1077.5	1443.0	1696.7	1894.5	2057.6	2196.8
140	1398.7	1881.4	2218.9	2483.6	2703.0	2890.9
H = 1000						
80	324.5	436.3	514.4	575.8	626.6	670.1
100	764.8	1040.3	1327.0	1393.7	1525.3	1639.3
120	1136.0	1152.7	1852.6	2092.9	2295.9	2472.6
140	1468.4	2013.0	2407.0	2724.1	2992.6	3227.1
H = 3000						
80	342.2	469.5	561.9	636.5	699.8	755.1
100	796.3	1101.2	1325.3	1507.8	1664.1	1801.8
120	1177.0	1632.7	1969.4	2244.8	2481.3	2690.3
140	1516.7	2108.1	2546.4	2905.8	3215.1	3488.9
H = 10^{15}						
80	351.3	487.5	588.3	670.8	741.8	804.6
100	812.1	1133.1	1372.6	1570.1	1740.9	1892.7
120	1197.2	1674.0	2031.1	2326.4	2582.2	2810.1
140	1540.2	2156.6	2619.2	3002.4		

Freon

Half Cone Angle = 3 °

RPM T_s	600	1200	1800	2400	3000	3600
H = 50						
80	155.1	164.4	168.6	171.1	172.7	173.9
100	437.4	472.3	488.5	498.3	505.0	509.9
120	704.2	767.9	798.1	816.4	829.0	838.4
140	960.3	1054.8	1100.2	1128.0	1147.2	1161.5
H = 100						
80	250.7	279.9	294.3	303.31	309.6	314.3
100	674.5	772.9	824.0	856.8	290.1	897.8
120	1060.7	1231.0	1321.7	1380.6	1423.0	1455.3
140	1422.9	1666.1	1797.9	1884.3	1946.9	1994.9
H = 500						
80	463.0	591.5	673.4	733.4	780.4	818.9
100	1127.4	1469.7	1696.0	1866.2	2002.5	2115.9
120	1697.0	2230.9	2589.3	2861.9	3082.2	3267.0
140	2212.0	2923.5	3406.0	3775.6	4076.1	4329.4
H = 1000						
80	512.7	677.6	789.4	875.0	944.7	1003.4
100	1221.9	1638.6	1928.8	2155.6	2343.1	2503.4
120	1823.2	2459.7	2907.8	3260.8	3554.6	3807.2
140	2362.4	3200.6	3794.0	4263.9	4656.7	4995.7
H = 3000						
80	550.9	747.4	887.4	998.6	1091.7	1172.3
100	1291.8	1769.8	2115.8	2394.3	2630.3	2836.4
120	1915.2	2634.2	3158.2	3582.3	3941.1	4259.5
140	2472.7	3409.4	4094.9	4651.6	5126.6	5544.0
H = 10^{15}						
80	571.5	786.9	944.2	1071.8	1180.4	1275.9
100	1328.4	1841.2	2220.1	2530.1	2796.3	3031.5
120	1962.7	2727.9	3295.8	3762.0	4163.6	4519.4
140	2528.5	3520.3	4258.5	4866.0	5390.2	5855.5

BIBLIOGRAPHY

1. Baker, H. D., Ryder, E. A., and Baker, N. H., Temperature Measurement in Engineering, Vol. 2, Wiley and Sons, New York, 1961.

2. Ballback, L. J., The Operation of a Rotating Wickless Heat Pipe, M.S. Thesis, Naval Postgraduate School, Monterey, California, December 1969.

3. Daley, T. J., The Experimental Design and Operation of a Wickless Heat Pipe, M.S. Thesis, Naval Postgraduate School, Monterey, California, June 1970.

4. Gebhart, B., Heat Transfer, 2d. Ed., McGraw-Hill, 1971.

5. Newton, W. H., Jr., Performance Characteristics of Rotating, Non-Capillary Heat Pipes, M.S. Thesis, Naval Postgraduate School, Monterey, California, June 1971.

6. Sparrow, E. M. and Hartnett, J. P., "Condensation on a Rotating Cone," Journal of Heat Transfer, Vol. 83, Series C, No. 1, pp 101-102, February 1961.

INITIAL DISTRIBUTION LIST

		No. Copies
1.	Defense Documentation Center Cameron Station Alexandria, Virginia 22314	2
2.	Library, Code 0212 Naval Postgraduate School Monterey, California 93940	2
3.	Professor P. J. Marto, Code 59Mx Department of Mechanical Engineering Naval Postgraduate School Monterey, California 93940	2
4.	Department of Mechanical Engineering, Code 59 Naval Postgraduate School Monterey, California 93940	1
5.	Lieutenant Commander John S. Woodard 899 Broadway Alameda, California	1

DOCUMENT CONTROL DATA - R & D

(Security classification of title, body of abstract and indexing annotation must be entered when the overall report is classified)

1. ORIGINATING ACTIVITY *(Corporate author)* Naval Postgraduate School Monterey, California 93940	2a. REPORT SECURITY CLASSIFICATION Unclassified 2b. GROUP

3. REPORT TITLE
The Operation of Rotating Non-Capillary Heat Pipes

4. DESCRIPTIVE NOTES *(Type of report and inclusive dates)*
Master's Thesis; March 1972

5. AUTHOR(S) *(First name, middle initial, last name)*
John Sanford Woodard

6. REPORT DATE March 1972	7a. TOTAL NO. OF PAGES 62	7b. NO. OF REFS 6
8a. CONTRACT OR GRANT NO.	9a. ORIGINATOR'S REPORT NUMBER(S)	
b. PROJECT NO.		
c.	9b. OTHER REPORT NO(S) *(Any other numbers that may be assigned this report)*	
d.		

10. DISTRIBUTION STATEMENT

Approved for public release; distribution unlimited.

11. SUPPLEMENTARY NOTES	12. SPONSORING MILITARY ACTIVITY Naval Postgraduate School Monterey, California 93940

13. ABSTRACT

A Nusselt-type analysis was performed for laminar film condensation on the inside of a truncated rotating cone, which included the interfacial shear between the vapor and condensate, the vapor pressure drop, the thermal resistance in the condenser wall, and the condenser exterior cooling mechanism. An approximation of this analysis made it possible to find a numerical solution for small half cone angles greater than zero. A parametric study was performed of this approximate solution for various fluids, RPMs, half cone angles, and exterior heat transfer coefficients.

A non-capillary rotating heat pipe containing distilled water as the working fluid was tested. It was rotated at 700, 1400, 2100, and 2800 RPM, and heat transfer rates of the heat pipe were determined experimentally for different vapor saturation temperatures corresponding to electrical power inputs ranging from 1 Kw to 7 Kw.

The experimental results showed that the heat pipe performance was influenced by non-condensible gases in the working fluid and suggested that the analytical solution predicted heat transfer rates which were too high.

4 KEY WORDS	LINK A		LINK B		LINK C	
	ROLE	WT	ROLE	WT	ROLE	WT
Heat Pipe						
Film Condensation						
Heat Transfer						

134429
Thesis
W835
c.1
Woodard
The operation of rotating non-capillary heat pipes.